Identifying and Assessing the Yield Implications of Forest Canopy Gaps in Forest Management Using Full Feature LiDAR

by

Daniel Edward Jensen

A thesis submitted in partial fulfillment of the requirements for the degree of

Master of Science

in

Forest Management and Biology

Department of Renewable Resources
University of Alberta

Abstract

Gaps in the forest canopy are common in boreal aspen, spruce and mixedwood stands and can negatively affect forest volume. Data from four Alberta Vegetation Inventory (AVI) polygons, two aspen (*Populus tremuloides*) and two white spruce (*Picea glauca*), were analysed to determine how forest volume is affected by the presence of forest canopy gaps and to determine if this approach could be used to reconcile stand volumes estimated by growth models with volumes obtained from ground samples. LiDAR point clouds were processed to create canopy height models (CHMs) for each polygon to differentiate canopy cover from canopy gaps. Strong curvilinear relationships were found between LiDAR gap area and expanded gap area measured in the stands ($R^2 > 0.90$). Based on the estimated expanded gap areas, the potential volume loss due to gaps in each polygon was assessed. Potential polygon volume was estimated by determining the average tree occupancy area for canopy trees within fully stocked areas of each polygon and then estimating the "missing" volume based on the number of trees required to fill the gaps. By comparing the estimates of volume lost to gaps to the potential polygon volume when the gaps were filled, it was shown that gaps affect volume by upwards of 18%. However, the effect of gaps on volume was variable between polygons. Lastly, the CHMs were combined with wet areas maps depicting depth to water index. Estimates of the effects of hydrology on gap size and frequency were calculated with results showing that gaps are larger and more frequent in poorly drained soils than they are in well drained soils.

Acknowledgements

I would like to thank my supervisor, Dr. Mike Bokalo, for giving me the opportunity to work as his graduate student. Your guidance and encouragement over this period of study provided a framework that allowed me to take this project beyond my highest expectations.

I would like to thank my co-supervisor, Dr. Phil Comeau and my committee members, Dr. Barry White and Dr. Glen Armstrong for their assistance in clarifying the direction of this research and for their feedback on the manuscript. I would also like to thank Dr. Scott Nielsen for acting as external examiner and for his comments on the manuscript.

This research would not have been possible without the funding and data provided by Alberta Environment and Sustainable Resource Development and Weyerhaeuser Grande Prairie. I would like to thank Kirk Johnson and Gabriel Oltean for their assistance in collecting field data in less than ideal conditions. I would also like to acknowledge the logistic support provided by Cosmin Tansanu, and technical support provided by Bev Wilson, Michal Pawlina, Jae Ogilvie, Rick Pelletier, Mike Abley and Ian Paine. I would like to acknowledge the members of the Western Boreal Growth and Yield Association for their support of this project and feedback on the value of these applications in industry. I would like to thank Alberta Pacific Forest Industries Inc. for providing the opportunity to test these methods at the landscape level.

I would like to acknowledge the members of the SIS Lab and the Comeau research group who have been both friends and colleagues over the course of this project.

Finally, I would like to thank my family for their support as I completed this project. This would not have been possible without your support and understanding.

Table of Contents

List of Tables

List of Figures

Chapter 1: Introduction

Gaps in the forest canopy are common in boreal aspen, spruce and mixedwood stands and can negatively affect forest volume since they do not contain merchantable trees. However, the ability to quantify the effects of canopy gaps on volume is not well developed. Permanent sample plots (PSPs) have traditionally been used to estimate forest growth, and are also used in modelling to predict how regenerating stands will grow. With the placement of PSPs being biased towards fully stocked stands, the effects of not considering gaps can lead to an overestimation of volume compared to whole stand estimates (Eriksson, 1967). To account for the presence of gaps, photo interpretation is often used at the landscape level (Alberta Sustainable Resource Development, 2005) and field sampling for gaps has been used in some instances to assess gaps at the stand level (BC Ministry of Forests, 1998). However, with photo interpretation being inexact and the cost of field sampling being high, complete enumeration using remote sensing techniques may be the best way to account for gaps (Tansanu, 2007).

With Light Detection and Ranging (LiDAR) now being widely available, the use of canopy models derived from LiDAR allows for complete enumeration of gaps within forest stands (Gaulton and Malthus, 2010). From these models, gap dimensions and areas can be determined and inferences about how these gaps affect forest volume can be made. Additionally, other information such a soil drainage data (Murphy et al., 2011), may be used in conjunction with these canopy models to determine the nature of individual gaps beyond what is available from canopy models alone. The use of these models has the potential to provide more data about forest canopy gaps than was previously available and has the potential to be used in decision making for both forest planning and operations. The purpose of the research presented in this thesis is to test a series of methods that can be used to process LiDAR from the raw point cloud into a format that can be easily interpreted and merged with other GIS layers so that the nature of forest gaps can be interpreted.

In Chapter 2, LiDAR point clouds for four Alberta Vegetation Inventory (AVI) polygons are processed to create canopy height models (CHMs). From these CHMs the polygons are classified into tracts of contiguous canopy cover or canopy gaps based on the return height from the LiDAR. A random sample of the gaps in each polygon was measured in the field to confirm that the gaps detected were present. From these measurements, statistical models are developed that predict expanded gap area (Runkle, 1982) from the LiDAR gap measured in the CHMs.

In Chapter 3, the CHMs developed in Chapter 2 are used along with estimates of expanded tree occupancy to classify individual gaps as either gaps that can host merchantable

trees or interstitial spaces that are too small to host merchantable trees. Using the merchantable gaps, the number of trees and the associated volume that could potentially be hosted in each merchantable gap is estimated. These estimates of lost volume, along with estimates of average polygon volume from temporary sample plot measurements, are then used to estimate the potential polygon volume. To ensure that our estimates are reasonable, these estimates of potential volume are then reconciled against volume estimates from fully stocked areas in each polygon.

In Chapter 4, wet areas mapping is introduced as a tool that can be used in conjunction with CHMs to determine how ground water affects forest canopy gaps. By combining each CHM with a map of the depth to water index (Murphy *et al.*, 2011); new raster models are created which quantify the local drainage class for each gap. From these raster models, the prevalence of gaps and the mean gap size for each drainage class is determined. Based on these results, inferences are made about how wet areas affect canopy gaps and how this knowledge can be used in forest planning and operations.

In Chapter 5, the results of each study are summarized, some general conclusions are provided about how the techniques used in this thesis can be applied, and suggestions about potential directions of future research are made.

References

Alberta Sustainable Resource Development. 2005. Alberta vegetation inventory interpretation standards. Version 2.1.1. Alberta Sustainable Resource Development, Resource Information Management Branch.

BC Ministry of Forests. 1998. OAF1 Project Report #2. Ground-based survey method. B.C. Ministry of Forests, Forest Practices Branch. Victoria, B.C.

Eriksson, H. 1962. A comparison between the yield figures for permanent sample plots and those for the stand as a whole. Royal College of Forestry, Department of Forest Yield and Research. Research Notes Nr:14. 72 pp. Printed in Swedish with English summary.

Gaulton, R., and Malthus, T.J. 2010. LiDAR mapping of canopy gaps in continuous cover forests: A comparison of canopy height model and point cloud based techniques. International Journal of Remote Sensing 31(5): 1193 – 1211. doi: 10.1080/01431160903380565

Murphy, P.N.C., Ogilvie, J., Men, F.-R., White, B., Bhatti, J.S., and Arp, P.A. 2011. Modelling and mapping topographic variations in forest soils at high resolution: A case study. Ecological Modelling **222(14):** 2314 – 2332. doi: 10.1016/j.ecolmodel.2011.01.003

Runkle, J.R. 1982. Patterns of disturbance in some old-growth mesic forests of eastern North America. Ecology **63(5)**: 1533–1546. doi: 10.2307/1938878

Tansanu, C.S. 2007. The Role of Forest Stand Structure in Predicting Yield. M.Sc Thesis. University of Alberta. 129 pp.

Chapter 2: The Application of LiDAR in Estimating Forest Canopy Gaps in the Boreal Forest

2.1 Introduction

The presence of gaps within the forest canopy can be natural or anthropogenic occurrences. Canopy gaps are areas where the height of the forest canopy is noticeably lower than adjacent areas (Runkle, 1992). Within a gap, canopy trees may be regenerating and growing, non-tree species such as shrubs, herbs or grasses may be suppressing canopy recovery, or growth may be absent due to poor growing conditions. With canopy gaps having the potential to affect harvest yields, estimation of their size and distribution can be useful to foresters.

Although a difference in canopy height is the key characteristic which defines a gap, a threshold for gap closure or a minimum gap area can also be part of the definition depending on the application. For example, in tropical forests Brokaw (1982) considered gaps to be closed when the understory reached 2 meters in height, while in temperate forests Runkle (1982) considered a gap closed when the understory had reached 10 – 20 meters in height. MacIssac *et al*. (2006) required a minimum area of 100 m^2 when looking at post-harvest regeneration. This requirement was set so that gaps present in harvested stands would be also discernible on aerial photos as the trees matured. When considering animal habitat, Fuller (2000) required at least 3 fallen trees and one gap axis to be at least 40 meters long, while Fukui *et al.* (2011) used gaps as small as 2 m^2 when surveying bats. With the definition of a gap being dependent on the application, a wide variety of definitions can be found.

Gaps can range in size from small interstitial spaces between trees that are too small for mature trees to occupy, to large patches caused by disturbance events. With disturbance events often causing drastic changes to the forest ecosystem, research involving gaps larger than 1000 m^2 often falls under disturbance research (Schliemann and Bockheim, 2011). For smaller gaps, the gap phase is often a temporary phase in the forest cycle, with a distinct event such as a tree fall resulting in *gap birth*. Gaps can also be persistent, unable to grow canopy trees, due to site conditions such as rock outcroppings or wet areas (BC Ministry of Forests, 1998). *Gap death* occurs when the gap becomes indistinguishable from the surrounding canopy, either through natural ingress or through the expansion of the crowns of bordering canopy trees.

Through a description of tree death as a forest process, Franklin *et al*. (1987) show that gap formation from the death of one or a few trees results in a wide variety of ecological changes. These include: a release of resources such as light, nutrients and moisture (Denslow *et al*., 1990);

the creation of new resources for wildlife habitat in the form of snags and coarse woody debris (Bouget and Duelli, 2004); and structural changes to other trees and forest soils when trees break or fall (Kuuluvainen, 1994). Among the research topics investigated that are related to gaps, those focusing on biodiversity and forest structure are most prevalent. Studies in biodiversity have included research on bryophyte diversity (Jonsson and Esseen, 1990), bat assemblages (Fukui *et al*., 2011), beetle assemblages (Bouget and Duelli, 2004), bird distributions (Fuller, 2000) and plant diversity (Chavez and MacDonald, 2010).

Beyond studies focusing on biodiversity, there has also been extensive research on the role gap formation and dynamics play as an aspect of forest structure. Watt (1947) was among the first to recognize the importance of gaps as part of forest structure when he identified the opening of gaps in the canopy as a phase in the forest growth cycle in beech forests. He determined that the gap phase is the period where canopy regeneration occurs, whereas in other phases of the growth cycle regeneration is excluded due to canopy or ground cover. Other researchers identified similar phases in other forest types such as maple-basswood forests in North America (Bray, 1956). As the gap phase became an accepted phase of the forest cycle, more research into the dynamics of individual gaps began. Beginning in the late 1970's, research into the gap dynamics was conducted in both tropical forests (Brokaw, 1982; Brokaw, 1985) and temperate forests (Runkle, 1982). Within the boreal regions, most research in gaps and gap dynamics has occurred in Scandinavian and Russian forests, and only limited research has occurred within the Canadian boreal forest (McCarthy, 2001).

In the Canadian boreal forest, early research on the gap phase of the forest cycle was indirect as the focus of the research was on processes of stand succession and the creation of gaps was identified as the mechanism which allowed understory release to occur. This is seen in aspen stands where decadent stands will slowly break up and the increase in light will allow for supressed understory species to emerge (Peterson and Peterson, 1992). More recent studies have focused directly on gaps with much of the research focusing on patterns of regeneration within gaps. Kneeshaw and Bergeron (1998) were among the first to survey gaps to evaluate the gap size distribution and determine patterns of mortality and recruitment. In Alberta, Cumming *et al.* (2000) showed that trembling aspen *(Populus tremuloides* Michx.) stands, which appear to be even aged, are actually uneven aged. They noted that the maintenance of continuous canopy cover occurs through the emergence of aspen suckers in newly formed gaps which grow to reach the canopy. Gaps can also release other tree species to encourage the formation of mixed forests. When aspen stands have white spruce (*Picea glauca* (Moench) Voss) in the understory, the gaps formed during the gap phase (break up) offer an opportunity for the understory spruce to enter the

canopy and create mixed stands (Cumming *et al*., 2000). MacIssac *et al.* (2006) showed that after harvest, gap area increased from pre-harvest levels. These increases can be mostly attributed to suppression of the regenerating canopy trees by competition and browsing. It was also shown that many gaps were likely persistent. These gaps were present pre-harvest and continued to be present as the stand developed. Tansanu (2007) conducted a study of the effects of forest canopy gaps on volume estimation. In his study, aerial photo interpretation and temporary sample plots were used to estimate the effects of gaps on volume estimation.

When gaps are newly formed, they are distinct canopy openings and there is very little understory ingress or crown expansion from bordering canopy trees to obscure the dimensions of the gap. As time passes, the dynamic nature of gaps adds temporal complications to measurements as ingress and crown expansion can make identifying the boundaries of gaps subjective. To account for this, Runkle (1982) suggested expanding gap measurements beyond the true canopy gap to the stems of the canopy trees bordering the gap. This *expanded gap* concept removes uncertainty regarding the translation of true gap edges from the canopy to the ground by using the bordering tree stems as gap vertices. This reduces the subjectivity of measurements and makes them easier to reproduce. The use of this concept also provides a better estimate of the area available for understory ingress, as saplings can establish anywhere within an expanded gap, not just in the true gap.

When working at the stand or landscape level, sampling gaps presents a challenge due to their random occurrence and variable size. Runkle (1982) presented a transect method for sampling canopy gaps which has been used in several studies in the Canadian boreal forest (*e.g*. Kneeshaw and Bergeron, 1998; Cumming *et al*., 2000). However, for studies at scales larger than a single forest stand, the transect method may not be intensive enough and too localized to allow for sufficient sampling. As an alternative to transects, MacIssac *et al.* (2006) used a time sequence of aerial photographs for select forest polygons and limited his selection of gaps to those greater than 100 m^2 to collect a large sample of gaps, and then conducted field measurements to validate his findings (MacIssac *et al*., 2006). In another study, Tansanu (2007) used photos interpreted to 10% canopy cover levels, along with intensive temporary sample plot measurements to determine the effects of gaps on volume estimates. Tansanu's methods yielded inconclusive results and suggested that complete enumeration would be required to determine the effects of gaps on forest volume estimates (Tansanu, 2007). One method of remote sensing that has shown promise in the delineation and complete enumeration of forest gaps is the use of Light Detection and Ranging (LiDAR).

Since the mid 1990's remote sensing technology has evolved to provide new tools for measuring and monitoring biospatial data (Reutebuch *et al*., 2005). LiDAR is an active remote sensing technology that works by directing light pulses from a source to a target. When the light is intercepted by a surface, part of the light pulse is reflected back towards a sensor at the source. By measuring the return time from pulse release to the return at the sensor, the distance from the source to the target can then be calculated. When LiDAR hardware is mounted on an aircraft, landscapes can be scanned during flights and large amounts of data can be collected in a short amount of time. Using the cloud of points that is collected, related points such as those that reflect solely off of the forest canopy can be grouped. From these groups of points, neighbouring points can be used to create surface models including raster models and triangulated irregular networks (TINs).

Among the surfaces that can be modelled, digital elevation models (DEMs) of the bare earth surface and canopy height models (CHMs) of the forest canopy are common products. Treitz *et al*. (2012) were able to accurately estimate a variety of forest properties including average stand height, top height, DBH, basal area, density, gross total volume, gross merchantable volume, and biomass using a 20 m × 20 m resolution raster model. In addition to tree characteristics, gap characteristics have also been estimated for a variety of forest types using LiDAR scans. To estimate canopy gaps in a forest stand, a CHM can be used. By correcting each pixel within the raster for local topography by subtracting the DEM surface elevation from the orthometric scan height determined during the LiDAR scan a height above ground level (a.g.l.) can be assigned. Pixels can then be classified as part of the canopy or as gaps by comparing the a.g.l. height to a gap/canopy threshold value that is determined by a gap definition. Using these models, proportions of gap and canopy pixels can be calculated, and groups of like pixels can be used to determine the dimensions of individual gaps. Among prior studies, Koukoulas and Blackburn (2004) investigated the use of LiDAR to extract gap features in oak forests in England. Vepakomma *et al*. (2008) used multi-temporal LiDAR data to identify gaps and estimate changes over time for boreal forests in Quebec, Canada. Gaulton and Malthus (2010) compared estimates from raster CHMs to estimates directly interpreted from the point cloud. Vehmas *et al*. (2011) used LiDAR to detect gaps in Finnish boreal forests and determine understory characteristics based on the hits found within the LiDAR gaps.

In this chapter previous studies are built upon by using LiDAR to estimate gap dimensions for two pure aspen and two mixed white spruce polygons in the boreal forests of Alberta, Canada. A gap definition is developed that includes forest volume as a key criterion. LiDAR scans are used to develop CHMs and then using this volume based definition these

models are used to estimate the total gap area and the distribution of gaps by area for each polygon. Predictive models are presented that use LiDAR gap areas to estimate expanded gap area. This chapter concludes by discussing the issues relating to the use of these methods and its significance.

2.2 Methods

2.2.1 Study Area and Research Polygons

Research was conducted in the Weyerhaeuser Grande Prairie forest management area (FMA). The southern portion of this FMA is approximately 60 km south of Grande Prairie, Alberta and consists of approximately 225,000 hectares of boreal mixedwood forest (Figure 2.1). In 2006, Tansanu (2007) conducted a study on forest fragmentation which attempted to link yield to canopy cover. The initial study selected twelve aspen (*Populus tremuloides* Michx.) and ten white spruce (*Picea glauca* (Moench) Voss) Alberta Vegetation Inventory (AVI) polygons. These polygons were further stratified into 10% canopy cover classes using photo interpretation. Each stratum was intensively sampled using temporary sample plots. From these 22 polygons, two aspen and two white spruce polygons were selected that had good access, had current aerial photography, and recent LiDAR point cloud data. The polygon names and locations, using both latitude and longitude coordinates and the Alberta Township System are presented in Table 2.1. For all polygons the final three digits of the AVI GISLink number corresponds to Tansanu's polygon numbers, with the exception of polygon number 411 which had a GISLink number of 6566412.

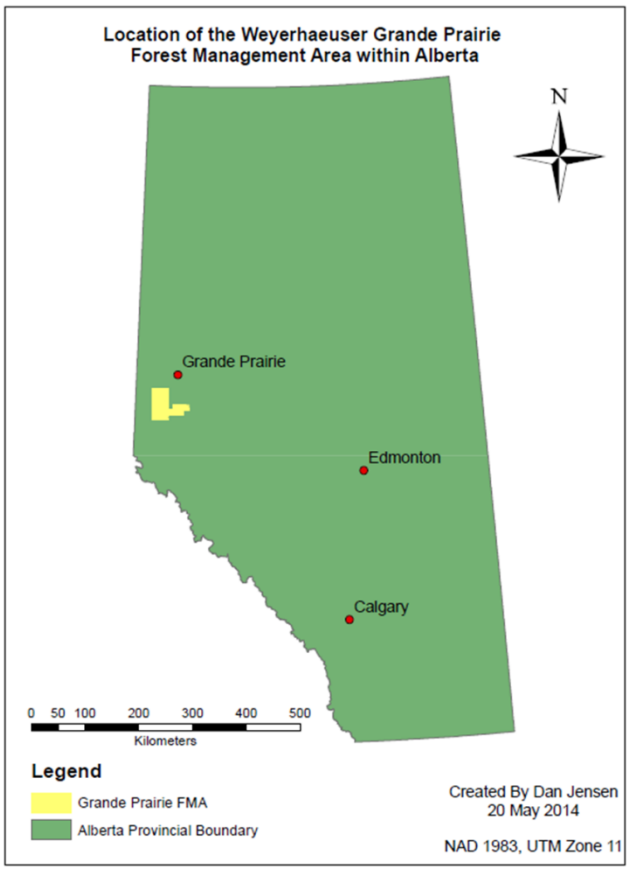

Figure 2.1: Location of the Weyerhaeuser Grande Prairie Forest Management Area within Alberta, Canada.

Table 2.1: Latitude and longitude coordinates for the centroids, and Alberta Township System locations of the Alberta Vegetation Inventory polygons used in this study.

Polygon GISLink #	Leading Species	Latitude	Longitude	Alberta Township System Legal Land Description (Legal Sub. - Sec. - Twp. - Rge. - Meridian)
6796103	Aspen	N54.7667	W119.3143	3 – 04 – 67 – 09 - W6
6866289	Aspen	N54.8712	W119.1494	8 – 09 – 68 – 08 - W6
6566412	White Spruce	N54.6408	W118.8840	9 – 19 – 65 – 06 - W6
64106639	White Spruce	N54.6527	W118.7575	8 – 25 – 64 – 10 - W6

2.2.1.1 Aspen Polygon Characteristics

The initial selection criteria used by Tansanu (2007) for aspen polygons was based on the following photo interpreted (AVI) criteria: pure aspen polygons (>80% of the stand canopy cover is aspen or balsam poplar), C density (51 – 70% total canopy cover), stand heights between 19 and 23 meters and a minimum polygon size of 10 hectares. In this study, Polygon 6796103 had a mesic moisture class, C density canopy cover, a stand height of 20 meters, a species composition of 80% aspen and 20% balsam poplar (*Populus balsamifera* L.) by canopy cover, a stand origin of 1920, and a timber productivity rating of medium. Polygon 6886289 had a mesic moisture class, a stand height of 22 meters, C density canopy cover, a species composition of 100% aspen,

a stand origin of 1910 and a timber productivity rating of medium. The original AVI classification type call, the weighted photo interpreted canopy cover percentage based on the 10% canopy cover classes described in Section 2.2.1, and the mean height (m), percent species composition based on volume and breast height age (years) from the temporary sample plot (TSP) cruise results for the selected stands are presented in Table 2.2 (Tansanu, 2007).

Table 2.2: The Alberta Vegetation Inventory and field sampled (TSP) polygon characteristics (height (m), species composition (%), and breast height age (years)) for the two sampled aspen polygons.

	Polygon 6796103	Polygon 6866289
AVI Classification	mC20Aw_8Pb_2 20-M	mC22Aw_{10} 10-M
Weighted Percent Canopy Cover based on air photos	70%	62%
Height (m) (TSP)	24.2	25.7
Percent Species Composition by Volume (TSP)	Aw 70%, Pb 30%	Aw 100%
Breast Height Age (years) (TSP)	87	97

2.2.1.2 White Spruce Polygon Characteristics

The initial selection criteria used by Tansanu (2007) for white spruce polygons was based on the following photo interpreted (AVI) criteria: white spruce dominant (>60% of stand composition by canopy cover), C density (51 – 70% of total canopy cover), stand heights between 19 and 27 meters and a minimum polygon size of 10 hectares. White spruce dominant stands were selected, because pure white spruce polygons (>80% of composition by canopy cover) were unavailable. Polygon 6566412 had a mesic moisture class, C density canopy cover, a stand height of 19 meters, a species composition of 70% white spruce, 10 percent lodgepole pine (*Pinus contorta* Dougl. ex Loud. var. *latifolia* Engelm.), 10 percent balsam fir (*Abies balsamsea* (L.) Mill.) and 10 percent aspen by canopy cover, a stand origin of 1910 and a timber productivity rating of medium. Polygon 64106639 had a mesic moisture class, C density canopy cover, a stand height of 22 meters, a species composition of 70% white spruce and 30% lodgepole pine by canopy cover, a stand origin of 1900 and a timber productivity rating of medium. The original AVI classification type call, the weighted photo interpreted canopy cover percentage based on the 10% canopy cover classes described in Section 2.2.1, and the mean height (m), percent species composition based on volume and breast height age (years) from the temporary sample plot (TSP) cruise results for the selected polygons are presented in Table 2.3 (Tansanu, 2007).

Table 2.3 The Alberta Vegetation Inventory and field sampled (TSP) polygon characteristics (height (m), species composition (%), and breast height age (years)) for the two sampled white spruce polygons.

	Polygon 6566412	Polygon 64106639
AVI Classification	$mC19Sw_7Pl_1Fb_1Aw_1$ 10-M	$mC22Sw_7Pl_3$ 00-M
Weighted Percent Canopy Cover Based on Air Photos	68%	54%
Height (m) (TSP)	18.1	22.7
Percent Species Composition by Volume (TSP)	Sw 70%, Pl 10%, Fb 10%, Pb 10%	Pl 50%, Sw 40%, Fb 10%
Breast Height Age (years) (TSP)	47	111

2.2.2 LiDAR Data

LiDAR point cloud data was acquired through the Resource Information Management Branch (RIMB) of the Alberta Ministry of Environment and Sustainable Resource Development (AESRD). This LiDAR dataset was collected over a four year period. The mean return density varied between the polygons, ranging between 1.25 hits/m^2 and 2.05 hits/m^2 across the four polygons. For the deciduous polygons, the flight for Polygon 6796193 occurred during October 2005 while the flight for Polygon 6886289 occurred during July 2007, meaning there is a difference in seasonality between these polygons. For the individual polygons, flight specifications and point cloud statistics are shown in Table 2.4.

Table 2.4: LiDAR flight data for the polygons used in this study.

	Polygon 6566412	Polygon 6796103	Polygon 64106639	Polygon 6886289
Cover Type	White Spruce	Aspen	White Spruce	Aspen
Flight Date	October 2003	October 2005	August 2006	July 2007
LiDAR Scanner Make and Model	Optech Altm 3100	Optech Altm 3100	Optech Altm 3100	Optech Altm 3100
Average Flight Altitude	990	1300	1250	1200
Pulse Rate	*	50 KHz	50 KHz	50 KHz
Scan Angle	*	25 Degrees	25 Degrees	25 Degrees
Flight Line Spacing	*	~500 meters	~500 meters	~500 meters
% Flight Line Overlap	*	50%	50%	50%
Planned Pulse Sample Spacing	*	0.5 to 0.6 hits	0.5 to 0.6 hits	0.5 to 0.6 hits
Mean Return Density (hits/m^2)	1.25	1.84	1.45	2.05
Standard Deviation of return density	0.44	0.52	0.64	0.69
Minimum Return Density	0.04	0.04	0.04	0.04
Maximum Return Density	2.72	4.72	4.80	5.24
Percentage of Data with return density between 1 and 3 hits/m^2	72.52	94.11	73.95	85.79

* This information was unavailable.

2.2.3 Analysis Methods

2.2.3.1 Differentiating Gaps from Canopy Cover

Raw LiDAR data was acquired as tiles spanning approximately 2.1 km × 2.4 km (500 ha) and was processed using the Fusion/LDV software package (McGaughey, 2014). When the coverage for a polygon consisted of multiple tiles, the tiles were processed to create a single

seamless coverage. The data were scanned using the "Catalog" script and checked visually for point cloud outliers, mainly for extreme height values. A digital elevation model (DEM) depicting the bare earth features was created using the "GroundFilter" and "GridSurfaceCreate" scripts. The "GroundFilter" was completed using 6 iterations and a 5 m × 5 m cell size. These parameters were used as it resulted in smoother surface interpretations than the default parameters when visually inspected. The "GridSurfaceCreate" was also completed using a 5 m × 5 m cell size and the "/minimum" switch was used so that the lowest point within the pixel was used to determine the surface elevation.

The points not classified as ground points were then corrected to the DEM to create a canopy height model (CHM) using the "CanopyModel" script (Appendices 1 and 2). The cell size for the CHM was set at 3 m × 3 m and the "/ground" switch was used so that the CHM would display the above ground level height values. Using this script, the maximum height within each pixel is used to classify the height. This removes bias towards underestimating the true pixel height (Naesset, 1997). The CHM was then converted to an ASCII raster file using the "DTM2ASCII" script prior to it being imported to ArcGIS 10.1 (ESRI, Redlands, California). Examples of the Fusion/LDV batch scripts used to create the DEMs and CHMs are presented in Appendix 2.1.

In ArcGIS 10.1, the CHM was clipped to the AVI polygon boundaries. Each pixel within the clipped raster was then reclassified using the ArcGIS "reclassify" tool as a gap or canopy pixel using a species specific merchantable height threshold. The merchantable heights of mature trees for both aspen and white spruce were predicted from height-diameter equations using a minimum stump diameter of 13 cm, which is a common pulpwood utilization standard for determining merchantable logs. For the 13 cm utilization standard, a merchantable height of 14.95 m was estimated for aspen and 12.07 m for white spruce. All pixels with values equal or greater than this threshold were considered to be part of the merchantable canopy and pixels below this threshold were considered gaps in the canopy.

Using the ArcGIS "raster to polygon" tool, groups of like pixels (gap or canopy) were then grouped based on pixel adjacency into simplified polygons to create a vector layer. These vector layers became the base dataset used to discriminate the gap areas from the canopy areas. Vectors were used instead of rasters as it creates smooth edges of the CHM gap boundaries and simplifies complex groups of pixels in to single objects. This conversion also allows for easier calculation of the areas of gaps or continuous canopy. These gap vector polygons derived using the LiDAR point cloud data are referred to as LiDAR gaps.

2.2.3.2 GIS Analysis

For each raster and vector CHM, the total polygon areas as well as the gap and canopy cover fractions within each polygon were calculated. This was done to determine how converting LiDAR data from a point cloud to a raster CHM and then to a vector CHM affects the interpretation of the edges of each polygon and the gap and canopy fractions. Additionally, a frequency distribution by gap area for each vector CHM was plotted in a histogram. This was done to show that these distributions had similar inverse J-shaped distributions to those seen in transect sampling (Kneeshaw and Bergeron, 1998). Gaps were categorized logarithmically as there were many small gaps and a few exceptionally large gaps in each polygon.

2.2.3.3 Measuring Gap Extents

With a focus on determining the relationship between LiDAR gap area and the area of gaps as they appear in the forest, a range of gaps were sampled in each of the AVI polygons. Gaps were stratified by area and then randomly selected within each stratum using the polygon numbers assigned in the creation of the vector CHM and a random number generator. For the two aspen polygons 68 LiDAR gaps were selected; 35 gaps in polygon 6886289, and 33 in polygon 6796103 were randomly selected. For the two spruce polygons 102 gaps were selected; 38 gaps in polygon 6566412 and 64 in polygon 64106639. Gaps with boundaries that extended beyond the AVI polygon boundaries were not included in the sample as it was too difficult to determine the actual AVI polygon boundaries in the field.

The centroid of each gap polygon was converted to a latitude and longitude coordinate and used as a GPS waypoint so that each target gap could be located in the field. Once located, the expanded gap for each of the selected LiDAR gaps was delineated (Runkle, 1982). To do this, the boundaries of the LiDAR gaps were expanded to also include the area from the edge of the gap to the stems of the nearest canopy trees to obtain the expanded canopy gap area (Appendix C). This approach was used as it overcomes the dynamic nature of gaps by reducing the subjectivity of the gap boundaries. To mark the gap extents, stems were flagged along the gap boundary and these locations were then recorded as GPS waypoints using a mapping grade GPS (Trimble GeoXT 6000). For each waypoint, 50 hits were recorded with the desired precision being between 1 and 2 meters when possible. To ensure that waypoint collection had minimal interference from the aspen canopy, the collection was done during the leaf off stage. Seasonality had no effect on waypoint collection in the white spruce polygons.

After data collection was completed, each waypoint was differentially corrected using the Cansel base station in Grande Prairie to improve the precision of each point location. The corrected waypoints of the individual tree locations bordering the LiDAR gap were then used as vertices to create a vector layer of polygons representing the expanded gaps. These expanded gaps were then overlaid on the original LiDAR gap layer (Appendix B). Each expanded gap and its associated LiDAR gap were visually confirmed in ArcGIS 10.1. In some cases, the expanded gap boundaries included more than one LiDAR gap. This occurred in cases where it was difficult to determine the gap boundaries in the field, or when the conversion from raster CHM to vector layer resulted in the creation of multiple polygons for a single expanded gap. To account for this, multiple LiDAR gaps were only considered to be associated with the expanded gap measured if the LiDAR gap centroids were contained within the expanded gap polygon. Once expanded gaps and the associated LiDAR gaps had been confirmed, expanded gap area and the total LiDAR gap area for each measured gap was calculated

2.2.3.4 Scatter Plots and Regression Analysis

The expanded gap areas measured in the field were plotted against the LiDAR gap areas from the vector models to graphically illustrate the relationship between the expanded gaps and the LiDAR gaps. The nature and strength of the relationship was then explored using linear and non-linear regression. Data analysis was completed using SAS 9.4 (SAS Institute, Cary N.C). Two models were fit for each polygon, a simple linear model (2.1) and a curvilinear power function (2.2). The model forms are:

$$Y = a + bx \qquad (2.1)$$

$$Y = a + bx^c \qquad (2.2)$$

where (Y) is the expanded gap in m^2, (x) *is* the LiDAR gap area in m^2, and (a), (b) and (c) are estimated coefficients. In the linear model (a) represents the y-intercept, a constant that represents the size of an expanded gap when the LiDAR gap size is 0. This value is related to the minimum area required to host a merchantable tree within each polygon. The second coefficient (b) affects the slope of the curve and depicts the rate of change between LiDAR gap and expanded gap. In the power function (a) represents the y-intercept, which has the same effect on the function as it does on the linear function. The second coefficient (b) is a scaling factor that moves the function up or down depending on the value of (x^c). The exponent (c) determines the rate of growth or decay for the function and the shape of the function.

For each model, the Y-intercept values were set based on estimates of tree crown area (7.11 m^2 for Polygon 6796103, 6.93 m^2 for Polygon 6886289, and 6.75 m^2 for the spruce polygons). The methods for determining these values are discussed in detail in Chapter 3. For both model types, the 1:1 line indicates that the expanded gap is the same size as the LiDAR gap. To evaluate the fit of the models I compared R^2 values, with higher values indicating a better fit; and RMSE, with lower values indicating a better fit.

2.3 Results

2.3.1 Aspen Polygons

2.3.1.1 GIS Analysis

For polygon 6796103, the estimated total area for the polygon is 65.49 hectares based on the AVI. The clipping of the LiDAR point cloud to these boundaries followed by the conversion to a raster CHM resulted in no change to the polygon area. The conversion from raster CHM to vector CHM then decreased the polygon area by 0.05 hectares resulting in a final area loss from the original AVI area by 0.05 hectares (0.07%). The conversion from raster CHM to vector CHM also resulted in changes to the amounts of area classified as gaps or canopy. The raster CHM had a total gap area of 22.96 ha and a total canopy area of 42.52 ha, while the vector CHM had a total gap area of 21.87 ha and a total canopy area of 43.57 ha, a change in area between the two models of 1.7%.

For polygon 6886289, the estimated total area is 27.56 hectares based on the AVI. The clipping of the point cloud to these boundaries followed by the conversion to a raster CHM resulted in an increase in polygon area by 0.1 ha (0.04%). The conversion from raster CHM to vector CHM decreased the polygon area to 27.54 hectares resulting in a final area loss of approximately 0.02 hectares (0.07%). The conversion from raster CHM to vector CHM also resulted in changes to the amounts of area classified as gaps or canopy. The raster CHM had a total gap area of 3.85 ha and a total canopy area of 23.72 ha, while the vector CHM had a total gap area of 3.61 ha and a total canopy area of 23.93 ha, a change in area between the two models of 0.9%. The results of the area comparisons for both polygons are shown in Table 2.5.

Table 2.5: Comparisons of the total polygon area and gap/canopy fractions for the aspen polygons between the Alberta Vegetation Inventory, raster canopy height model (3 m × 3 m cell size and vector canopy height model areas.

	AVI	CHM Raster Model			CHM Vector Model		
Polygon Number	Polygon Area (ha)	Polygon Area (ha)	Gap Area (ha)	Canopy Area (ha)	Polygon Area (ha)	Gap Area (ha)	Canopy Area (ha)
6796103	65.49	65.49	22.96 (35.1%)	42.52 (64.9%)	65.44	21.87 (33.4%)	43.57 (66.6%)
6886289	27.56	27.57	3.85 (14.0%)	23.72 (86.0%)	27.54	3.61 (13.1%)	23.92 (86.9%)

With the creation of the vector CHM model from the 3 m × 3 m cell size raster models, descriptive statistics were calculated for the gap areas in both polygons (Table 2.6). For each polygon the frequency of gap sizes was plotted in a histogram (Figure 2.2 for Polygon 6796103 and Figure 2.3 for Polygon 6886289). The frequency distributions show an exponential decrease as LiDAR gap size increases. There are a high number of small gaps within each polygon and as the area increases the counts decrease. In both polygons there were a few exceptionally large gaps which are attributed to either anthropogenic disturbance (a well site in Polygon 6796103 and a cut line in Polygon 6886289) or to large areas within the polygon that were sparsely treed.

Table 2.6: Descriptive statistics of the gap areas for the aspen polygons in this study.

Polygon Number	Gap Count	Mean Gap Area (m^2)	Standard Deviation	Minimum Gap Area (m^2)	Maximum Gap Area (m^2)
6796103	3690	59.26	511.53	5.76	23991.00
6886289	612	59.04	450.89	5.76	10639.77

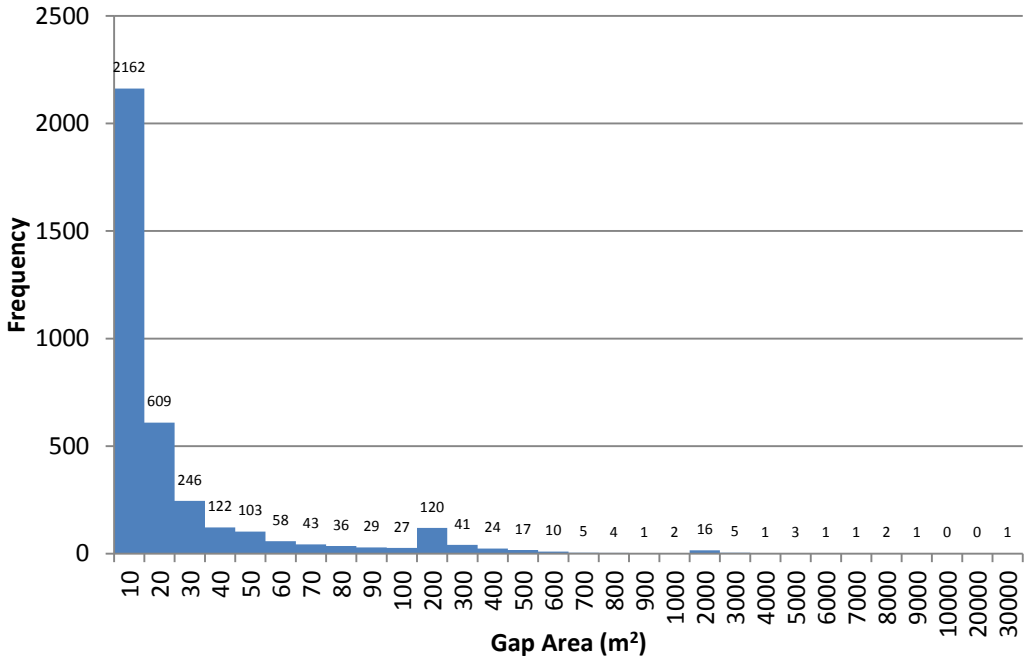

Figure 2.2: Frequency distribution of LiDAR gap sizes for Polygon 6796103.

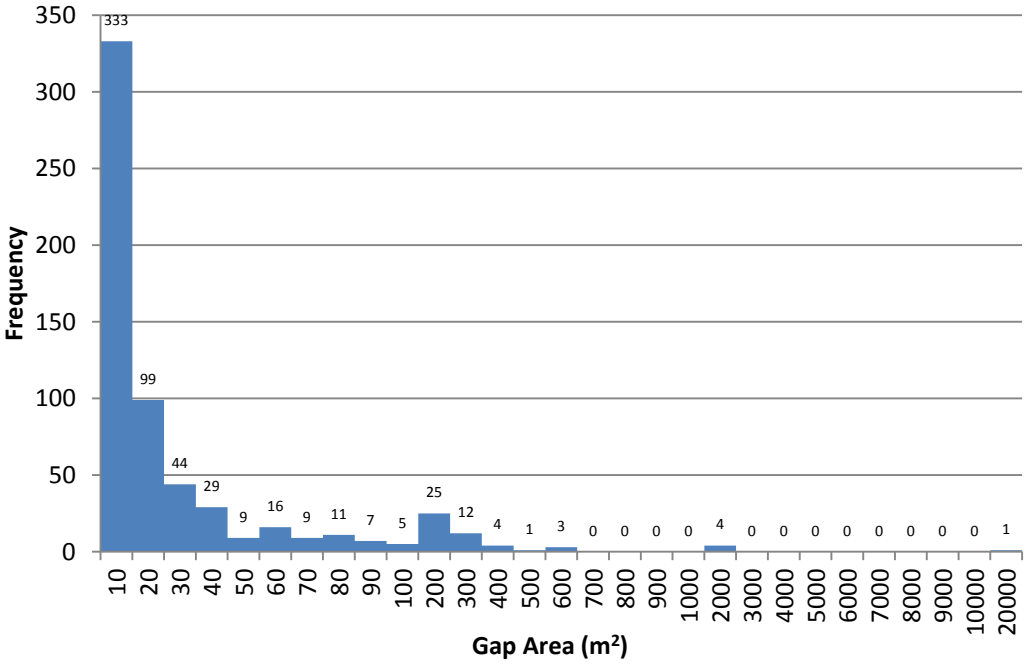

Figure 2.3: Frequency distribution of LiDAR gap sizes for Polygon 6886289.

2.3.1.2 Gap Extents

For each vector model of the CHM, estimated LiDAR gap areas were plotted against the corresponding expanded gap area measured in the field. Linear and power function models were then fit for each polygon using SAS 9.4.

For polygon 6796103, the linear model (2.3) was statistically significant ($p<0.001$, $R^2=0.894$, RMSE=116.88, n=33). The non-linear model (2.4) was also significant ($p<0.001$, $R^2=0.949$, RMSE=81.92, n=33). The models for this relationship are:

$$Y = 7.11 + 1.974x \quad (2.3)$$

$$Y = 7.11 + 21.613x^{0.567} \quad (2.4)$$

where (Y) is the estimated area of the expanded gap and (x) is the area of the LiDAR gap. For the linear model, the 95% confidence interval for the slope is 1.72 to 2.22. For the power function, the 95% confidence intervals are: 7.046 to 36.181 for the coefficient and 0.441 to 0.693 for the exponent.

For polygon 6886289, the linear model (2.5) was statistically significant ($p<0.001$, $R^2=0.832$, RMSE=202.24, n=35). The non-linear model (2.6) was also significant ($p<0.001$, $R^2=0.944$, RMSE= 118.40, n=35). The models for this relationship are:

$$Y = 6.93 + 3.379x \quad (2.5)$$

$$Y = 6.93 + 45.711x^{0.524} \quad (2.6)$$

where (Y) is the estimated area of the expanded gap and (x) is the area of the LiDAR gap. For the linear model, the 95% confidence interval for the slope is 2.84 to 3.92. For the power function, the 95% confidence intervals are: 24.017 to 67.404 for the coefficient and 0.431 to 0.618 for the exponent.

With the confidence intervals of the slopes for the two linear models not overlapping, the two models are significantly different; therefore pooling the data to create an aggregate model was not justified. For the power functions the confidence intervals between the two models overlap for both terms, however there is clear differentiation between the populations based on the seasonality of the LiDAR scans that does not advocate for pooling the data. When comparing the linear models and the power functions, the power function is a better representation of the relationship between LiDAR gaps and expanded gaps. This determination is based on the higher R^2 values and lower RMSE fit statistics for the dataset. A scatterplot of the linear and non-linear models are presented in Figure 2.4 and Figure 2.5.

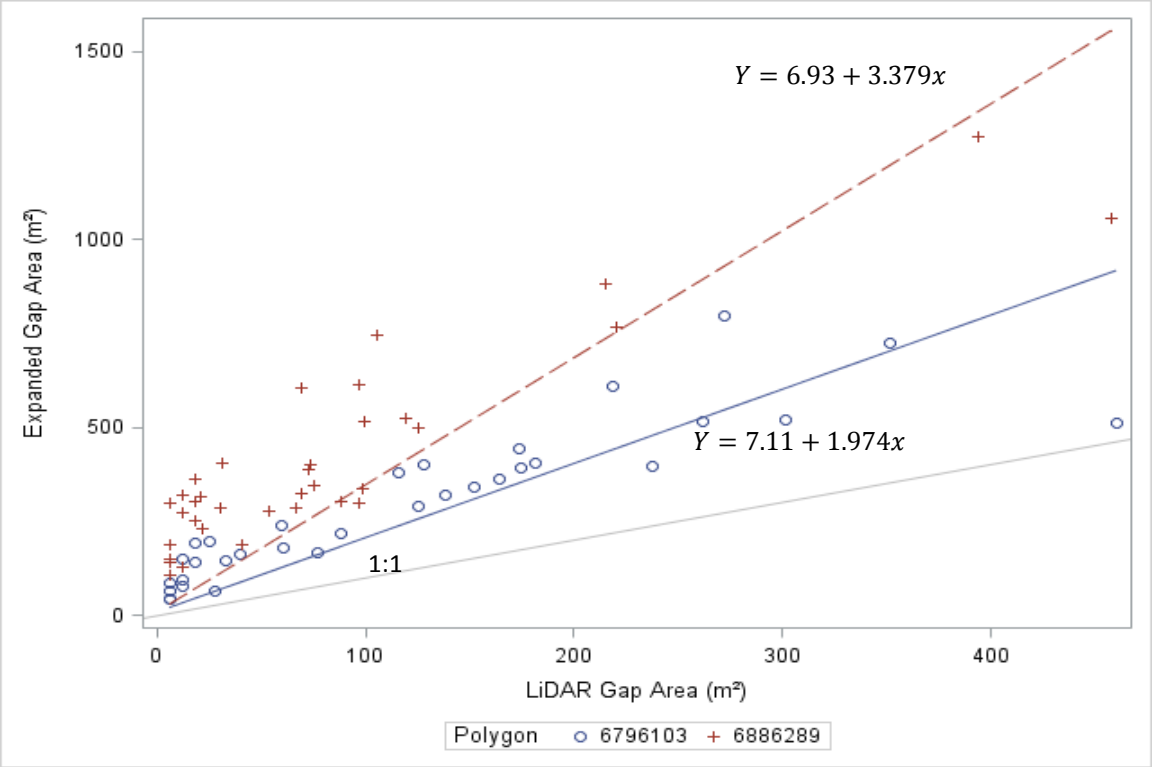

Figure 2.4: Relationship between LiDAR gap area and expanded gap area for aspen polygons using linear models. The models used for these relationships are Y= a + bX.

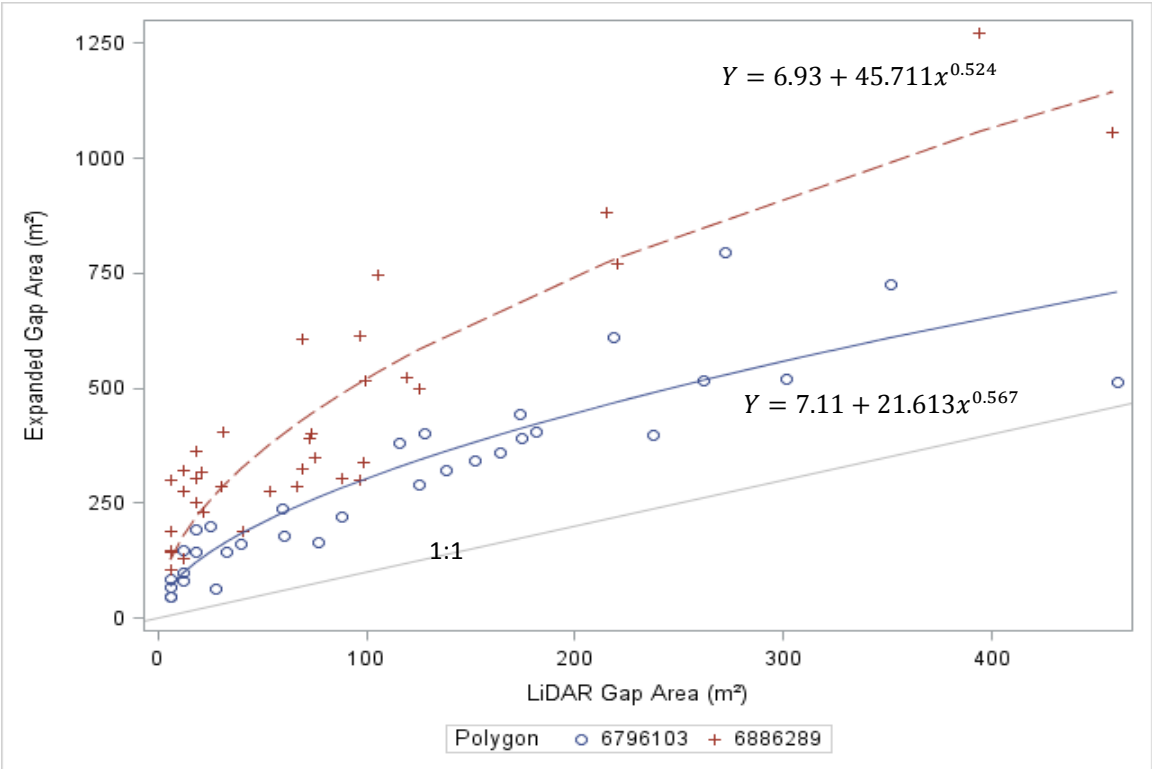

Figure 2.5: Relationships between LiDAR gap area and expanded gap area for aspen polygons using power function models. The models used for these relationships are $Y= a + bX^c$.

2.3.2 White Spruce Polygons

2.3.2.1 GIS Analysis

For polygon 6566412, the estimated total area is 12.86 hectares based on the AVI. The clipping of the point cloud to these boundaries followed by the conversion to a raster CHM resulted in no change to the polygon area. The conversion from raster CHM to vector CHM decreased the polygon area to 12.85 hectares resulting in an area loss of approximately 0.1 hectares (0.08%). The conversion from raster CHM to vector CHM also resulted in changes to the amounts of area classified as gaps or canopy. The raster CHM had 6.20 ha of gap area and 6.66 ha of canopy area, while the vector CHM had 6.06 ha of gap area and 6.79 ha of canopy area, a change of 1.09%.

For Polygon 64106639, the estimated total area is 51.53 hectares based on the AVI. The clipping of the point cloud to these boundaries followed by the conversion to a raster CHM resulted in a loss of 0.04 hectares (0.08%) to the area of the polygon. Part of this change can be attributed to the 11 pixels (99 m^2, 0.02%) in the raster CHM classified as "no data" pixels, due to a lack of point cloud hits within the pixel area. The conversion from raster CHM to vector CHM decreased the polygon area to 51.44 hectares resulting in a final area loss of approximately 0.05 hectares (0.10%). The conversion from raster CHM to vector CHM also resulted in changes to the amounts of area classified as gaps or canopy. The raster CHM had 15.40 ha of gap area and 36.09 ha of canopy area, while the vector CHM had 14.50 ha of gap area and 36.94 ha of canopy area, a change of 1.7%. These results are shown in Table 2.7

Table 2.7: Comparisons of the total polygon area and gap/canopy fractions for the white spruce polygons between the Alberta Vegetation Inventory, raster canopy height model (3 m × 3 m cell size), and vector canopy height model areas.

	AVI	CHM Raster Model			CHM Vector Model		
Polygon Number	Polygon Area (ha)	Polygon Area (ha)	Gap Area (ha)	Canopy Area (ha)	Polygon Area (ha)	Gap Area (ha)	Canopy Area (ha)
6566412	12.86	12.86	6.20 (48.2%)	6.66 (51.8%)	12.85	6.06 (47.2%)	6.79 (52.8%)
64106639	51.53	51.49	15.40 (29.9%)	36.09 (70.1%)	51.44	14.50 (28.2%)	36.94 (71.8%)

With the creation of the vector CHM from the 3 m × 3 m cell size raster model, descriptive statistics were calculated for the gap areas in both polygons (Table 2.8). For each polygon, the frequency of gap sizes was in a histogram (Figure 2.6 for Polygon 6566412 and Figure 2.7 for Polygon 64106639). The distributions of gap areas are similar to the distributions shown in the aspen polygons. In Polygon 6566412, the largest gap is attributed to anthropogenic disturbance (a road) within the polygon. With many gaps bordering the road corridor, this gap was much larger than the estimated 1.3 hectares that could be attributed to just the road.

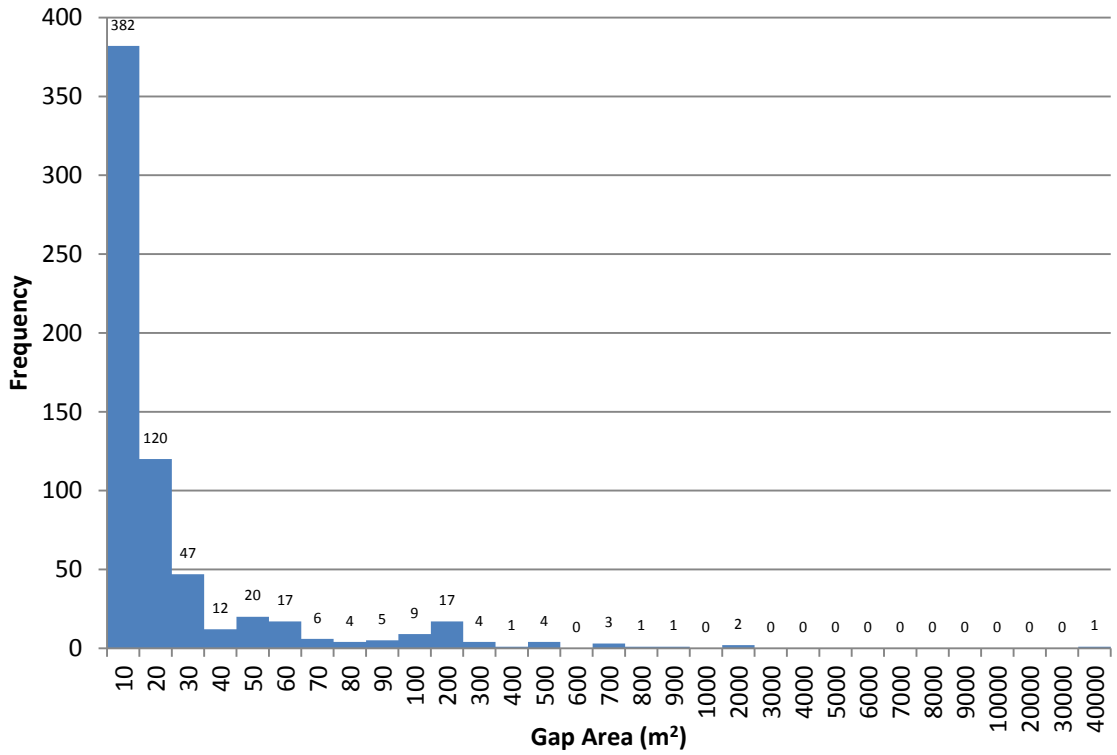

Figure 2.6: Frequency distributions of LiDAR gap sizes for polygon 6566412.

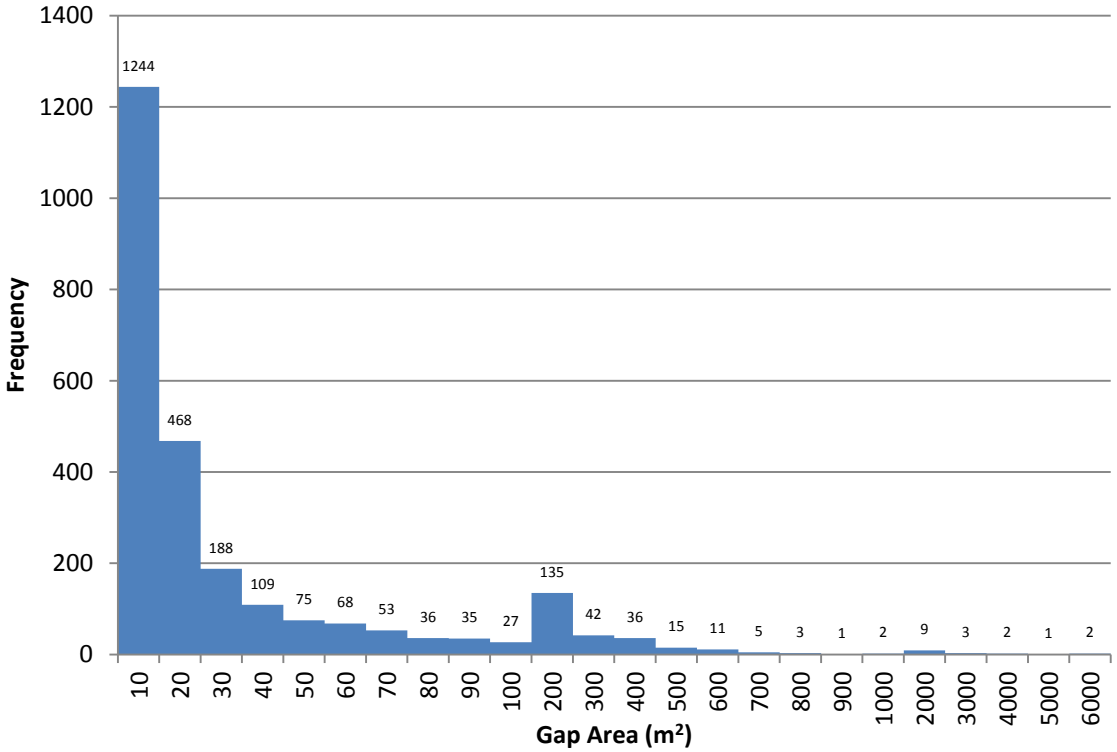

Figure 2.7: Frequency distribution of LiDAR gap sizes for polygon 64106639.

Table 2.8: Descriptive statistics of the gap areas for the white spruce polygons in this study.

Polygon Number	Gap Count	Mean Gap Area (m^2)	Standard Deviation	Minimum Gap Area (m^2)	Maximum Gap Area (m^2)
6566412	656	92.39	1527.26	5.76	39075.49
64106639	2570	56.53	244.10	5.76	5678.53

2.3.2.2 Gap Extents

For each vector model of the CHM, estimated LiDAR gap areas were plotted against the corresponding expanded gap area measured in the field. Linear and power function models were then fit for each polygon using SAS 9.4

For polygon 6566412, the linear model (2.7) was statistically significant ($p<0.001$, $R^2=0.826$, RMSE=54.94, n=33). The non-linear model (2.8) was also significant ($p<0.001$, $R^2=0.912$, RMSE=39.79, n=33). The models for this relationship are:

$$Y = 6.75 + 0.883x \quad (2.7)$$
$$Y = 6.75 + 12.944x^{0.499} \quad (2.8)$$

where (Y) is the estimated area of the expanded gap and (x) is the area of the LiDAR gap. For the linear model, the 95% confidence interval for the slope is 0.73 to 1.04. For the power function, the 95% confidence intervals are: 3.786 to 22.101 for the coefficient and 0.359 to 0.639 for the exponent.

For polygon 64106639, the linear model (2.9) was statistically significant ($p<0.001$, $R^2=0.850$, RMSE=109.66, n=65). The non-linear model (2.10) was also significant ($p<0.001$, $R^2=0.913$, RMSE=84.08, n=65). The models for this relationship are:

$$Y = 6.75 + 1.230x \quad (2.9)$$
$$Y = 6.75 + 15.183x^{0.587} \quad (2.10)$$

where (Y) is the estimated area of the expanded gap and (x) is the area of the LiDAR gap. For the linear model, the 95% confidence interval for the slope is 1.10 to 1.36. For the power function, the 95% confidence intervals are 7.970 to 22.395 for the coefficient and 0.505 to 0.669 for the exponent.

With the confidence intervals of the two models not overlapping, the linear models are significantly different from one another; therefore the pooling of the data to create an aggregate model was not justified. For the power functions, the confidence intervals between the two models overlap for both terms. When comparing the linear models and the power functions the power function is a better representation of the relationship between LiDAR gaps and expanded gaps. This determination is based on the R^2 and RMSE fit statistics for the dataset. A scatterplot of the linear and non-linear models are presented in Figure 2.8 and Figure 2.9.

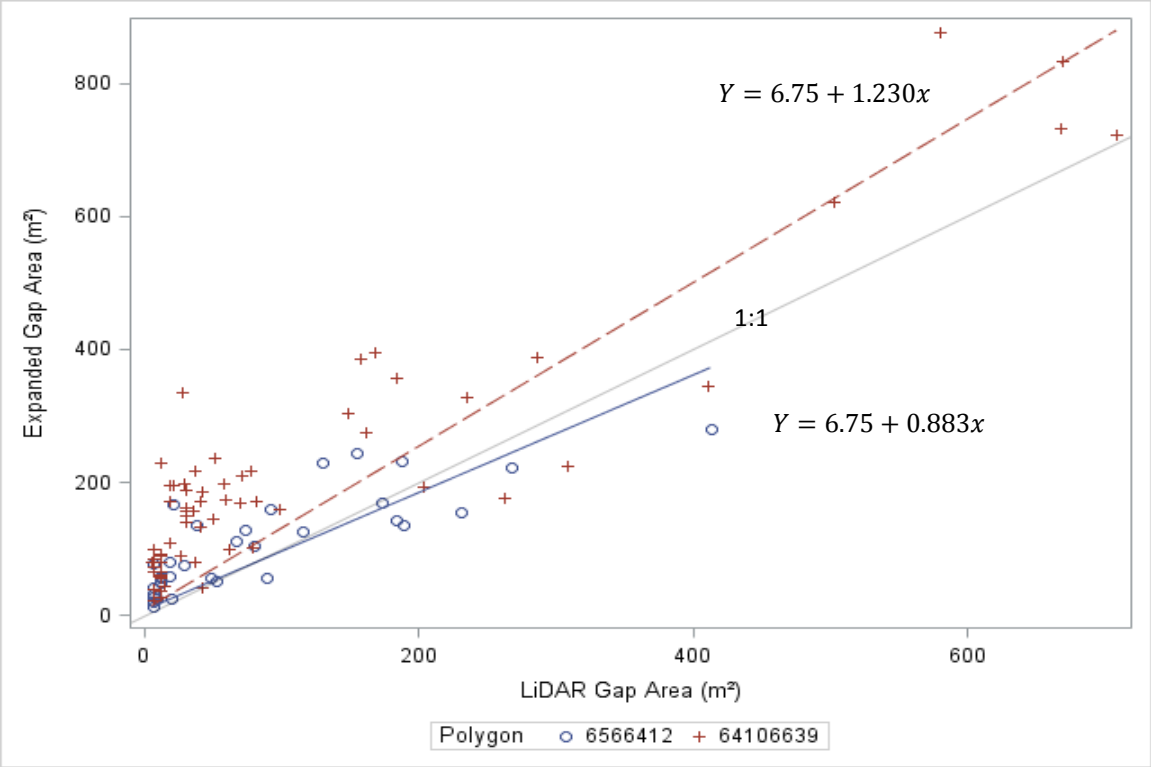

Figure 2.8: Relationships between LiDAR gap area and expanded gap area for white spruce polygons using linear models. The models used for these relationships are Y= a + bX.

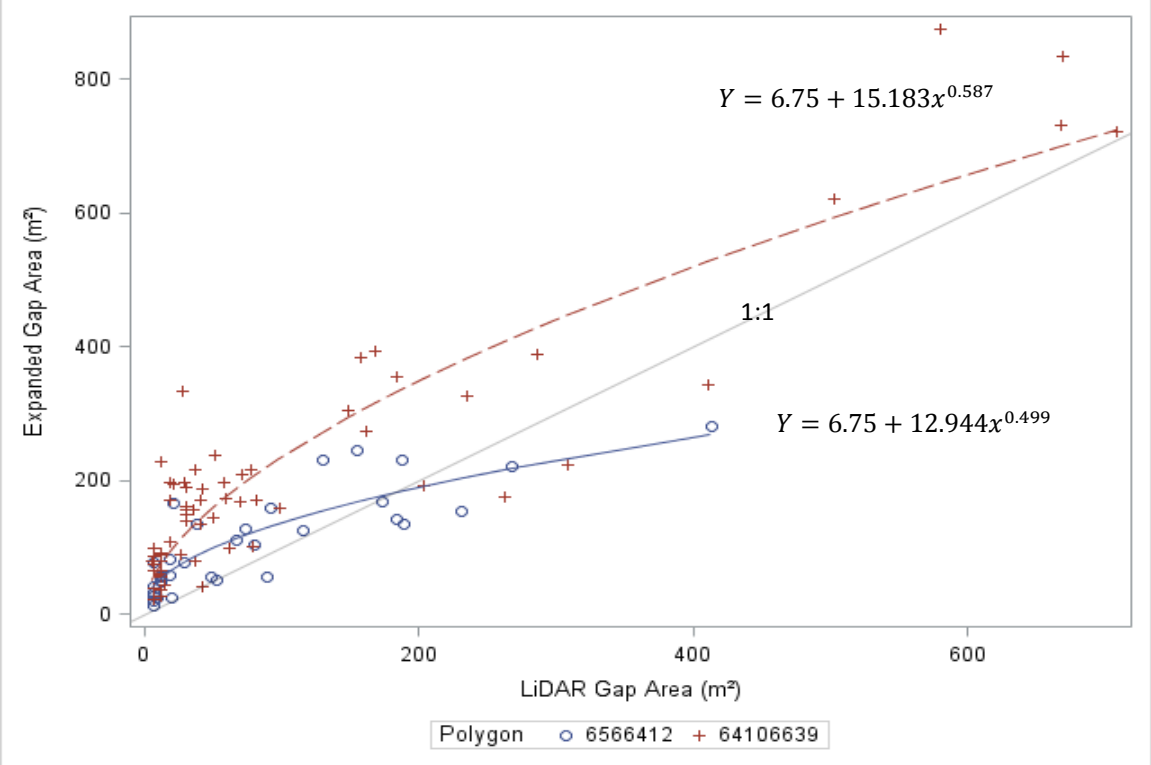

Figure 2.9: Relationships between LiDAR gap area and expanded gap area for white spruce polygons using power function models. The models used for these relationships are $Y= a + bX^c$.

2.4 Discussion

2.4.1 GIS Analysis

The LiDAR point cloud data that was used in this analysis had a hit density that averaged 1.7 hits/m^2 when weighted by polygon area. At this hit density, clipping the point cloud using AVI polygon boundaries and then converting the point cloud to a raster CHM and then vector CHM produced area and cover estimates that were very close to those delineated through photo interpretation. The differences in the total area estimates between AVI and the CHMs were small with none exceeding 0.08% of the total polygon area. This high correspondence shows that the hits were spread evenly throughout each polygon so there were no pixels within the polygon that lacked hits and that discrepancies were concentrated along the boundaries of each polygon.

When the polygons were initially selected for analysis, all had an AVI canopy cover class of C (50-70% canopy cover). From the vector CHMs, the only polygon that had a canopy cover estimate outside of this range was Polygon 6886289, an aspen polygon, which was calculated to be 86.9% canopy cover. With LiDAR interpretation being more objective than photo interpretation, discrepancies may be due to several issues. These include the gap definition and pixel size used for LiDAR interpretation, the challenges of photo interpretation in some polygons (Tansanu, 2007), the differences between the time the aerial photos were taken and the LiDAR scans were conducted, and the effects of converting a raster to a vector model.

The frequency distribution of gap sizes developed from the vectorized CHMs showed an inverse J-shaped distribution similar to those developed using traditional transect sampling. The distribution developed from the CHMs showed that interstitial spaces and small treefall gaps under 100 m^2 are ubiquitous throughout a polygon, with gaps of this size having a relative frequency of 92%, but making up only a small amount (7%) of the total polygon area. In contrast, larger gaps from disturbance events have a relative frequency of 8% within each polygon, but make up 22% of the total polygon area. This agreement of sampling distributions and population enumeration agrees with results obtained by Kneeshaw and Bergeron (1998) for aspen and conifer stands in Quebec.

2.4.2 Gap Analysis

With LiDAR gaps having dimensions that are not equal to the true canopy gap, the development of statistical models that relate LiDAR gaps to the expanded gap allows for better estimation of gap area in a polygon than LiDAR gaps alone would provide. To accurately measure gaps in the field, it required a methodology that was objective, replicable and could

verify that the use of LiDAR gaps was an appropriate surrogate to field measurements. To do this, the expanded gap concept presented by Runkle (1982) was used. By expanding the gap measurements beyond the canopy gap to the nearest tree stems it was possible to objectively identify the vertices of the gaps, whereas measuring the canopy gap directly was less objective. Also with the time between gap formation and the LiDAR scans and the time between the LiDAR scans and the field measurements spreading across several years, the expanded gap removes the effects of recent dynamic changes on the gaps. With the stems of the boundary trees being used as vertices, the expanded gap area would remain constant over time unless further disturbance or growth occurred. By developing both linear models and power functions to describe the relationship, much of the variation present in the data sets can be explained.

In the aspen polygons, the slope values provided by the linear functions most likely reflect differences in phenological stages of the polygons when LiDAR was flown. LiDAR was flown in October for Polygon 6796103 and July for Polygon 6886289. In Polygon 6796103, the slope of approximately 3.4 represents leaf off polygon, while in Polygon 6886289 a slope of 2.0 was determined for leaf on. The non-linear power functions illustrate similar relationships between the LiDAR gaps and expanded gaps, and also show the differences between two polygons that were seen in the linear models. The strength of using the power function over linear models is that as gap size increases, the difference between LiDAR gap area and expanded gap area tapers because the proportion of the total expanded gap area that would be measured underneath the crowns of the bordering trees becomes smaller than the area sensed by the LiDAR.

In the white spruce polygons, the linear functions were also less effective than the power functions at explaining the relationship between LiDAR gaps and expanded gaps. However, with the slope values of the linear functions being very close in value it shows that when phenology is not a factor that the relationships between LiDAR gaps and expanded gaps have similar trajectories across different polygons. With the conical crown shapes of white spruce, the relationship between LiDAR gap and expanded gap is closer to a linear relationship than seen in the aspen models. The narrower tree crowns and the lower and denser canopy also introduces error into the measurements as it is more difficult to collect GPS locations close to the stems of some trees. This is seen in the measurements of Polygon 6566412, where both the linear and power function curves have values that are lower than the 1:1 relationship between LiDAR gaps and expanded gaps. Further research is required to find methods that reduce the error seen when estimating expanded gap area in white spruce polygons.

2.4.3 Gap Definition

The frequency distributions and predictive models created are strongly influenced by the gap and pixel size criteria selected prior to analysis of the point cloud and field measurements. With the focus of this thesis on investigating how LiDAR can be used to fully enumerate canopy gaps with forest volume as an objective, it required a gap definition which was consistent with historical definitions relating to the height of the regenerating canopy (*e.g.* Brokaw, 1982; Runkle 1982), but also required a linkage to volume. To determine merchantable height, a 13 cm stump diameter was used as it is a common standard for merchantable pulpwood. From this stump diameter, a taper equation (Huang, 1994) was used to estimate tree heights. The tree heights estimated based on this stump diameter were used as threshold heights that were consistent with traditional gap definitions that were determined using volume criteria. By setting this merchantable height criterion as a threshold, all hits below the threshold were classified as being within gaps and all hits above as part of the forest canopy. With the threshold being definitive, hits can be classified as part of a gap regardless of whether they reflect off of the ground or unmerchantable biomass (*e.g.* saplings, shrubs).

2.4.4 LiDAR Biases

The potential biases that result from using LiDAR are present because the randomness of the pulses rarely results in hits that contact the canopy maxima of individual trees. If a raster is created to model the canopy surface and an arithmetic mean is used to estimate the canopy height for a pixel then the value will likely be an underestimate of the actual height (Naesset, 1997). Naesset suggests that if the maximum height within an individual pixel is used as the pixel height value and not an average then the estimate will be unbiased. While this method was used to account for bias in this study, other methods such as adjusting the merchantable height using LiDAR point cloud information for the area around the point could be used to limit the effects of this bias. If it is known how much the LiDAR is underestimating canopy height, then a polygon wide adjustment may also improve the canopy estimate. However, when comparing models across different cover types or adjusting values to mixed stands, this may not be effective since the correction factor will likely differ between conifer, deciduous, and mixed stands.

Using models other than rasters may also reduce biases. By directly interpreting gap dimensions from the point cloud, Gaulton and Malthus (2010) were able to accurately interpret gap edges using high density LiDAR scans. In this study, a raster method was chosen because it was a simpler surface than a TIN and with a simple canopy/gap surface being interpreted, the

texture of the surface was less important. Due to the low density of hits in our LiDAR data, use of the point cloud directly to interpret the surface would be unlikely to improve models. Using raster models instead of TINs or models created from point clouds also keeps the models simple to meet the objective of developing methods that are practical for forest planning using current technology and interpretable by all forest planners.

2.4.5 Determining Pixel Size

In choosing to use a raster model as a base for the CHM, the most important aspect is selecting an appropriate pixel size. For a given hit density, it is important to find a pixel size that is big enough to allow for accurate estimates of canopy height. At the same time, minimizing the number of pixels that have no hits, ensuring small gaps are not missed and ensuring that boundaries of the polygons are not over- or under-estimated to large extents are all considerations. Overall, pixel size defines what gaps are seen in the model and this is directly relates to point cloud density. With point cloud density being a major factor in determining the cost of the LiDAR scans, this also affects what pixel size is used. Treitz *et al.* (2010) conducted a study using dense scans and then decimated them to determine how the scans perform at lower density. Their results suggest that a scan density as low as 0.5 hits/m^2 for a 20 m × 20 m pixel can provide effective results for collecting forest inventory data. With scan densities in this study ranging between 1.25 and 2.05 hits/m^2, it is sufficient for this study and by setting the raster pixel size to 3 m × 3 m, it was possible to identify gaps in the field that were delineated by the raster model. A 3 m × 3 m pixel was chosen after visually assessing the canopy height models that were created with pixel sizes ranging from 2 m × 2 m to 10 m × 10 m. At this pixel size, identifying small gaps within the polygon was possible and the creation of large, contiguous gaps throughout each polygon was minimized.

To find an appropriate balance for pixel size, stand conditions must be taken into consideration. The selection of one deciduous polygon that was leaf on and one that was leaf off meant that there needed to be a balance that did not sacrifice precision in either case. When a deciduous polygon is leaf on the gaps are distinct, while leaf off polygons have very little discernible expanded gap. This is demonstrated in the linear regression models as the slope coefficient for Polygon 6886289, the leaf on polygon, is approximately 2.3 while in Polygon 6796103, the leaf off polygon, the slope coefficient is approximately 1.5. In leaf off polygons there are only stems and branches for the laser pulses to reflect off of, while in leaf on polygons the large amount of leaf biomass increases the reflective surface areas. This creates more distinct boundaries between gaps than in leaf off polygons and may allow for smaller pixels to be used.

This means that in leaf off situations, a larger pixel may be required compared to leaf on conditions and if scans across multiple seasons are being used then a larger polygon is the best option to minimize the effects of seasonality. Other stand characteristics, such as stand age and the presence or absence of more than one tree species, can also affect scans and affect which pixel sizes are the best options.

Another consideration that can affect the choice of pixel size are mixed stands of deciduous and conifer trees. With aspen trees having distinct crowns that are widest at the top and spruce having a conical shape with the maximum width approximately 2/3rds of the total tree height (Sattler *et al*., 2014), LiDAR is more likely to underestimate spruce than aspen. As a result, the use of larger pixels allows for better estimation of conifer heights as there are more hits per pixel to take the estimate from. When taking estimates for mixed stands, larger pixels may be preferable so that the conifer portions are not underestimated but this is done at the expense of more accurate measurements within the deciduous portions of the polygon. Overall, it is clear that pixel size is the most important issue in developing models of the forest canopy that consider gaps and that careful consideration of field conditions is required before developing models.

With the selection of a pixel size that accurately models canopy gaps, the raster models were then converted to vectors which simplified the model from a series of pixels into gap and canopy polygons. In doing this, gaps with dimensions that are more likely to appear in the forest were modelled. This conversion also allowed simplifies analysis as polygon centroids could be used for field navigation and areas of larger gaps were easier to determine. This conversion had the potential to add additional error to the LiDAR gap estimates as there was a conversion from point data to a raster and then a vector. When the area of the original AVI polygons to the raster and the vector areas we compared, there was very little change to the extents of the polygons, with the maximum difference being 0.02 ha. The conversions from raster to vector model created some discrepancies in the amount of canopy and gap area interpreted. Between the four AVI polygons the maximum difference in gap or canopy area between the raster and vector models was 3.6% in Polygon 6796103, while others did not exceed 1%. As the count of gaps increases the area discrepancy should be expected to increase as the amount of edge will increase and the smoothing of edges will result in loss of either gap or canopy area. Had the pixel resolutions been increased beyond 3 m × 3 m cell size then this would have resulted in more unclassified areas due to a lack of data, and likely reduced the ability of our models to predict field conditions.

2.5 Conclusions

The results from this chapter show that it is possible to model the dimensions and spatial distribution of forest canopy gaps in the Canadian boreal forest using canopy height models to the same degree as other regions (*e.g.* Koukoulas and Blackburn, 2004; Vepakomma *et al*., 2008; Gaulton and Malthus, 2010; Vehmas *et al*., 2011). Being able to completely enumerate gaps provides a variety of benefits including more accurate classification of canopy cover for forest inventory and the ability to monitor change to the forest canopy with the use of LiDAR scans over time. Further research in the area of mature tree occupancy may allow for improvement of these models by altering the Y-intercept values and the use of other data, such as wet areas maps, may allow for further classification of individual gaps into temporary and persistent types.

References

Alberta Sustainable Resource Development. 2005. Alberta vegetation inventory interpretation standards. Version 2.1.1. Alberta Sustainable Resource Development, Resource Information Management Branch.

BC Ministry of Forests. 1998. OAF1 Project Report #1: An overview of stocking gaps and OAF1 estimates for TIPSY. BC Ministry of Forests, Forest Practices Branch Victoria, BC.

Bouget, C., and Duelli, P. 2004. The effects of windthrow on forest insect communities: a literature review. Biological Conservation **118(3):** 281 – 299. doi: 10.1016/j.biocon.2003.09.009

Bray, J.R. 1956. Gap Phase Replacement in a Maple-Basswood Forest. Ecology **37(3):** 598 – 600. doi: 10.2307/1930185

Brokaw, N.V.L. 1982. The definition of treefall gap and its effect on measures of forest dynamics. Biotropica **14(2):** 158 – 160. doi: 10.2307/2387750

Brokaw, N.V.L. 1985. Gap-phase regeneration in a tropical forest. Ecology **66(3):** 682 – 687. doi: 10.2307/1940529

Chavez, V., and Macdonald, S.E. 2010. The influence of canopy patch mosaics on understory plant community composition in boreal mixedwood forest. Forest Ecology and Management **259(6):** 1067 – 1075. doi: 10.1016/j.foreco.2009.12.013

Comeau, P.G., Filipescu, C.N., Kabzems, R., and Delong, C. 2009. Corrigendum to: Growth of white spruce underplanted beneath spaced and unspaced aspen stands in northeastern B.C. – 10 year results. Forest Ecology and Management **257(7):** 1629 – 1636. doi: 10.1016/j.foreco.2009.01.025

Cumming, S.G., Schmiegelow, F.K., and Burton, P.J. 2000. Gap dynamics in boreal aspen stands: is the forest older than we think? Ecological Applications **10(3):** 744–759. doi: 10.2307/2641042

Denslow, J.S., Schultz, J.C., Vitousek, P.M., and Strain, B.R. 1990. Growth responses of tropical shrubs to treefall gap environments. Ecology **71(1):** 165 – 179. doi: 10.2307/1940257

Frankin, J.F., Shugart, H.H., and Harmon, M.E. 1987. Tree death as an ecological process. Bioscience **37(8):** 550 – 556. doi: 10.2307/1310665

Fukui, D., Hirao, T., Murakami, M., and Hirakawa, H. 2011. Effects of treefall gaps created by windthrow on bat assemblages in a temperate forest. Forest Ecology and Management **261(9):** 1546 – 1552. doi: 10.1016/j.foreco.2011.02.001

Fuller, R.J. 2000. Influence of treefall gaps on distributions of breeding birds within interior old-growth stands in Bialowieża Forest, Poland. The Condor **102(2):** 267 – 274. doi: 10.1650/0010-5422(2000)102[0267:IOTGOD]2.0.CO;2

Gaulton, R., and Malthus, T.J. 2010. LiDAR mapping of canopy gaps in continuous cover forests: A comparison of canopy height model and point cloud based techniques. International Journal of Remote Sensing **31(5):** 1193 – 1211. doi: 10.1080/01431160903380565

Huang, S. 1994. Report #1: Individual tree volume estimation for Alberta: Methods of formulation and statistical foundations. Alberta Environmental Protection, Land and Forest Service, Forest Management Division.

Jonsson B.G., and Esseen, P.-A. 1990. Treefall disturbance maintains high bryophyte diversity in a boreal spruce forest. Journal of Ecology: **78(4):** 924 – 936. doi: 10.2307/2260943

Kneeshaw, D.D., and Bergeron, Y. 1998. Canopy gap characteristics and tree replacement in the southeastern boreal forest. Ecology: **79(3):** 783 – 794. doi: 10.1890/0012-9658(1998)079[0783:CGCATR]2.0.CO;2

Koukoulas, S. and Blackburn, G.A. 2004. Quantifying the spatial properties of forest canopy gaps using LiDAR imagery and GIS. International Journal of Remote Sensing **25(15):** 3049 – 3071. doi: 10.1080/01431160310001657786

Kuuluvainen, T. 1994. Gap disturbance, ground microtopography, and the regeneration dynamics of boreal coniferous forests in Finland – a review. Annales Zoologici Fennici **31(1):** 35 – 51.

MacIsaac, D., Comeau, P.G., and Macdonald, S.E. 2006. Dynamics of regeneration gaps following harvest of aspen stands. Canadian Journal of Forest Research **36(7):** 1818 – 1833. doi: 10.1139/X06-077

McCarthy, J. 2001. Gap dynamics of forest trees: A review with particular attention to boreal forests. Environmental Reviews **9(1)**: 1 – 59. doi: 10.1139/er-9-1-1

McGaughey, R.J. Fusion/LDV – Version 3.41. Build Date Jan 28, 2014. United States Department of Agriculture - Forest Service, Pacific Northwest Research Center

Naesset, E. 1997. Determination of mean tree height of forest stands using airborne laser scanner data. ISPRS Journal of Photogrammetry & Remote Sensing **52(2):** 49 – 56. doi: 10.1016/S0924-2716(97)83000-6

Peterson, E.B., and Peterson, N.M. 1992. Ecology, management and use of aspen and balsam poplar in the prairie provinces, Canada. Forestry Canada, Northern Forestry Center. Special Report 1.

Reutebuch, S.E., Andersen, H.-E., and McGaughey, R.J. 2005. Light detection and ranging (LIDAR): an emerging tool for multiple resource inventory. Journal of Forestry **103(6):** 286 – 292.

Runkle, J.R. 1982. Patterns of disturbance in some old-growth mesic forests of eastern North America. Ecology **63(5)**: 1533–1546. doi: 10.2307/1938878

Runkle, J.R. 1992. Guidelines and sample protocol for sampling forest gaps. USDA Forest Service General Technical Report PNW-GTR-293.

Sattler , D.F., Comeau, P.G., and Achim, A. 2014. Branch models for white spruce (*Picea glauca* (Moench) Voss) in naturally regenerated stands. Forest Ecology and Management **325:** 74 – 89. doi: 10.1016/j.foreco.2014.03.051

Schliemann, S.A., and Bockheim, J.G. 2011. Methods for studying treefall gaps: A review. Forest Ecology and Management **261(7):** 1143 – 1151. doi: 10.1016/j.foreco.2011.01.011

Tansanu, C.S. 2007. The Role of Forest Stand Structure in Predicting Yield. M.Sc Thesis. University of Alberta.

Treitz, P., Lim, K., Woods, M., Pitt, D., Nesbitt, D., and Etheridge, D. 2012. LiDAR sampling density for forest resource inventories in Ontario, Canada. Remote Sensing **4(4):** 830 – 848. doi: 10.3390/rs4040830

Vehmas, M., Packalen, P., Matlamo, M., and Eerikainen, K. 2011. Using airborne laser scanning data for detecting canopy gaps and their understory type in mature boreal forest. Annals of Forest Science **68(4):** 825 – 835. doi: 10.1007/s13595-001-0079-x

Vepakomma, U., St-Onge, B., and Kneeshaw, D. 2008. Spatially explicit characterization of boreal forest gap dynamics using multi-temporal LiDAR data. Remote Sensing of Environment **112(5):** 2326 – 2340. doi: 10.1016/j.rse.2007.10.001

Watt, A.S. 1947. Pattern and Process in the Plant Community. Journal of Ecology **35 (1 and 2):** 1 – 22. doi: 10.2307/2256497

Appendix 2.1. Fusion/LDV Batch Scripts Used to Create DEMs and CHMs.

The following scripts were used to develop the raster models used in this thesis. Further documentation of these scripts is available in Fusion/LDV manual

Polyclipdata /shape:field#,value Polyfile OutputFile DataFile

Clips a .las file to the boundaries of an ESRI shapefile. Where: "/shape:field#,value" refers to the specific polygon used to clip the data; "Polyfile" refers to the directory location of the ESRI .shp file; "OutputFile" refers to the output .las file created from this process; and "DataFile" refers to the .las file that is to be clipped.

Catalog /image /index /coverage /intensity:area,min,max /density:area,min,max /firstdensity:25,1,3 /outlier datafile [catalogfile]

Creates a Fusion catalog file which provides descriptive reports for LiDAR data sets. Where "/image" creates an image file for the .las file; "coverage" creates an image showing the data coverage for the .las file; "/intensity" creates an intensity image using the intensity values for the point cloud where area is designated pixel area for the image, while min and max set the range of intensity values used for the image color ramp. For images used in this thesis area was set to 2, min was set to 0 and max was set to 186; "/density" and "/firstdensity" create images showing the density of LiDAR hits across the landscape with /density using all hits and /firstdensity only using first hits. Where area is the pixel area, and min and max set the color range for the optimal hit density. For images used in this thesis, area was set to 25, min was set to 1 and max was set to 3; "/outlier" creates a report that can identify height outliers; datafile refers to the raw .las file being catalogued; and [catalogfile] refers to the name of the output file. For this thesis catalogs were run for both the clipped .las file created from the "polyclipdata" script and for the group of unclipped .las files that intersect the target AVI polygon.

Groundfilter /iterations:# /diagnostics outputfile cellsize datafile

Filters the raw .las file using a filtering algorithm to create a .las of ground points. Where "/iterations:#" refers to the number of iterations used to develop the file; "diagnostics" provides diagnostic information during the run about the intermediate files created; "outputfile" refers to the name of the output file created; "cellsize" refers to the pixel size used to create the intermediate products; and "datafile" refers to the individual .las file or a .txt file listing multiple .las files that are being filtered.

GridSurfaceCreate /minimum surfacefile cellsize xyunits zunits coordsys zone horizdatum vertdatum datafile

Creates a surface model from a .las file, most frequently a bare earth digital elevation model (DEM). Where "/minimum" sets the minimum value within each pixel as the pixel elevation value; "surfacefile" refers to the output file that will be created from this script, which is in a .dtm format; cellsize refers to the pixel size of the product, which was set to 5 for this thesis; "xyunits and "zunits" refer to the units of the datafile which were both set to M for meters; "coordsys" refers to the coordinate system used which was set to 1 for UTM; "zone refers to the zone of the coordinate system which was 11; "horizdatum" and "vertdatum" refer to the horizontal and vertical datums that the datafile used which were set to 2 for NAD83 and 0 for unknown resepectively ; and "datafile" refers to the raw .las files used to create the surface, which in this case are were created using the Groundfilter script.

CanopyModel /ground:file Surfacefile cellsize xyunits zunits coordsys zone horizdatum vertdatum datafile

Creates a canopy surface model from a .las file. Where "/ground:file" refers to the DEM created from the GridSurfaceCreate script, using this switch results in a product that has been corrected for elevation; "surfacefile" refers to the output file that will be created from this script which is in a .dtm format; cellsize refers to the pixel size of the product, which was set to 3 for this; "xyunits and "zunits" refer to the units of the datafile which were both set to M for meters; "coordsys" refers to the coordinate system used which was set to 1 for UTM; "zone refers to the zone of the coordinate system which was 11; "horizdatum" and "vertdatum" refer to the horizontal and vertical datums that the datafile used which were set to 2 for NAD83 and 0 for unknown resepectively ; and "datafile" refers to the raw .las files used to create the surface.

DTM2ASCII inputfile [outputfile]

Converts .dtm files created by the GridSurfaceCreate and CanopyModel scripts into ascii files which can then be imported into ArcMap for further processing. "inputfile" refers to the .dtm files created by either the GridSurfaceCreate or CanopyModel script; and "[outputfile]" refers to the name of the output file created, which by default is an .asc file.

Chapter 3: Estimation of Forest Volume Lost to Gaps and Reconciliation of These Estimates Against Sampled Volume Estimates.

3.1 Introduction

Gaps in the forest canopy represent areas that are not stocked with trees and therefore do not contribute to total forest volume. In Alberta, MacIssac *et al*. (2006) attributed up to 29% of the area in regenerating aspen polygons to gaps, while Cumming *et al.* (2000) measured upwards of 16% gaps in mature aspen polygons. In Chapter 2, complete enumeration of gaps through LiDAR analysis resulted in average gap percentages of 23% in aspen polygons and 38% in white spruce polygons. With gap frequency varying by forest polygon and potentially affecting a large proportion of growing area, developing methods to account for the effects of gaps on polygon and landscape yields has the potential to improve short term yield estimates by adjusting yields to account for gaps and in long term forest planning by preventing overestimation of yield for future harvests.

Traditional forest volume estimates have come from a combination of permanent sample plots (PSPs) and temporary sample plots (TSPs). The establishment and repeated measurement of PSPs is used to develop growth curves for different forest strata. In some instances, such as in Alberta, AESRD government PSPs are biased towards fully stocked areas (Alberta Land and Forest Service, 1994). Data from these PSPs are used to estimate potential yield for a forest stratum and can be used to develop "normal" yield tables for a region. Adjusting normal yield tables according to local stocking levels is one way to account for gaps within a polygon. One issue with this approach is that a percent stocking adjustment is needed to use these normal yields in application. Biased placement means that the PSPs assume that the sampled polygon is more fully stocked and more homogeneous than is truly the case. In reality, forests in Alberta are heterogeneous polygons consisting of many biological stands (Tansanu, 2007). The effect of PSP bias on volume estimates was investigated by Eriksson (1964) in Swedish forests. In this study, volume estimates from PSP measurements were compared to whole stand volume estimates taken using randomly placed temporary sample plots. The results showed that PSPs had yields 15% higher than whole stand estimates.

In addition to PSPs, a random sample of TSPs is often used to estimate average stand volume. With random placement, TSPs provide a sample that includes the natural variability seen on the landscape and accounts for both species variability and the presence of gaps when the sample size is adequate. From this random sample, TSP data can be used to estimate volume for

large forest polygons, or be stratified by local conditions to create cover type volume tables. One weakness of TSP data is that a large sample is required to estimate volume, especially if there are a large number of strata, strata variability is high, or there is a large land base. In Alberta, TSPs are also often limited to natural stands since older managed stands are unavailable to sample. In these cases growth models are used to predict growth of these stands. Additionally, while random sampling may be sufficient for planning, the results may still have confidence intervals too wide for other uses.

With the emergence of LiDAR as a forest inventory tool, the ability to completely enumerate gaps is now possible, providing an alternative to field sampling methods. Through the creation of canopy height models, gaps can be enumerated and areas for each gap can be estimated (*LiDAR gap area*). From these LiDAR gap areas, expanded gap areas can be estimated using the relationships developed in Chapter 2. With LiDAR gap area being affected by tree crown overhang and seasonality (deciduous polygons); estimating the expanded gap (Runkle, 1982) area can be based on the relationship between LiDAR gap area and expanded gap area. This provides a more consistent estimate of ground area available to host trees while LiDAR gap area can help determine if there is sufficient area amongst the tree crowns for an additional tree. With knowledge of the crown area and expanded occupancy for trees in fully stocked areas, we can classify gaps which are large enough to host trees as *merchantable gaps*, and gaps that are too small as *interstitial space*.

The difficulty is to determine how much area a tree needs within a stand. With tree crowns showing plasticity, trees can respond to the opening of gaps by expanding their crowns into newly opened spaces. Conversely, as crowns expand their growth and size may be limited by the expansion of neighbouring trees. The actual area that trees need to grow varies by species, size, age and local growing conditions. Therefore, determining this area should be done on a stand by stand basis. When assessing the amount of area corresponding to a gap in the preceding chapter, we relied on the expanded gap (Runkle, 1982) to provide a consistent way of measuring the ground area associated to an opening in the canopy. To determine how much area a single canopy tree needs to compete, an expanded occupancy measurement can be used in the same way. By measuring trees in fully stocked areas, we can determine how much area canopy trees require and classify gaps of this size as merchantable gaps.

For each merchantable gap, volume lost to the gap can be estimated. The summation of the volume from all the gaps provides an estimate of total volume lost to gaps in a stand or polygon. To ensure that these estimates are reasonable, estimates of volume for an entire polygon (average polygon yield) and for fully stocked areas within that polygon (potential or normal

yield) can be obtained through TSP measurements. Since average polygon yields account for gaps, we can add the estimates of volume lost to gaps to the average polygon yields to produce an estimate of potential polygon yield. This value can then be compared to our estimates of normal yield to help determine if our estimates are reasonable.

The objectives of this chapter are to classify gaps defined in Chapter 2 using the vector CHM as merchantable gaps or interstitial space and to estimate the expanded occupancy area and crown area for trees in fully stocked areas of the polygon. Using these measurements we will estimate how many trees and how much volume is potentially lost to merchantable gaps within each polygon and reconcile this volume loss against estimates of normal yield taken from TSPs in the fully stocked areas of a polygon. The implications of our findings on yield will be discussed.

3.2 Methods

3.2.1 Expanded Occupancy Measurements

To estimate the mean expanded occupancy area for dominant and codominant trees in each polygon, sampling was conducted in three of the four Alberta Vegetation Inventory (AVI) polygons analysed in Chapter 2. The polygons sampled include the two aspen (*Populus tremuloides* Michx.) polygons (Polygons 6796103 and 6886289), and one white spruce (*Picea glauca* (Moench) Voss) polygon (Polygon 6566412). Polygon 64106639 was not included in this part of the study, because there were not enough large patches of contiguous white spruce to allow for sampling. In 2006, Tansanu sampled this polygon for volume using temporary sample plots (Tansanu, 2007). Since those data were collected, parts of this polygon had been sanitized to limit the spread of mountain pine beetle (*Dendroctonus ponderosae* Hopkins) during the recent outbreak in Alberta. This entailed cutting and burning lodgepole pine (*Pinus contorta* Dougl. ex Loud. var. *latifolia* Engelm.) infested with beetles. Sanitation did not affect the amount of white spruce in this polygon; however the removal of pine resulted in a reduction of canopy cover throughout the polygon which increased the difficulty in finding patches where white spruce could be sampled for the purpose of estimating the expanded occupancy. Sanitation did not affect gap delineation methods conducted in Chapter 2.

For the three polygons in which sampling occurred, air photo interpretation was used to stratify each AVI polygon into fragments based on 10% canopy cover classes (Tansanu, 2007). Fragments were assigned a value between 0 (0% to 10% canopy cover) and 9 (91% to 100% canopy cover) with no minimum fragment area requirement. The stratified fragment boundaries were imported into ArcGIS 10.1 (ESRI, Redlands, California) and used to delineate the AVI polygons. Fragments classed as 6 or greater (60% to 100% canopy cover) were identified as

candidates for sampling. Within each candidate fragment, a tie point was found near the fragment boundary and transects were overlaid starting at this point running parallel to the longest axis of the polygon. At approximately 30 meter intervals along each transect, a tree was selected for sampling to determine expanded occupancy area for the leading tree species (aspen or white spruce). A goal of 30 sampling points (individual expanded occupancy measurements) was set for each polygon. Each point was located in the field, and concentric circles were used to find the nearest dominant or codominant canopy tree of the leading species (*target tree*). For a target tree to be selected, it had to have a crown completely enclosed by other canopy trees (*boundary trees*) (Appendix D). To ensure independence from other points the target tree also had to be within 15 meters of the sampling point to ensure it did not share boundary trees with another target tree. For each target tree, the DBH was recorded and the target and boundary trees were mapped using a mapping grade GPS (Trimble GeoXT 6000) to record tree location. A minimum of 50 hits were recorded at a desired precision between 1 and 2 meters for each recording. If no tree met these criteria, then the point was rejected.

After sampling was completed, the GPS points collected for each target and boundary tree were differentially corrected and used to create polygons in ArcGIS 10.1. These polygons represented the expanded occupancy area for target trees. From these polygons, descriptive statistics for each of the target trees and their associated expanded occupancy area were calculated. For each AVI polygon, expanded occupancy areas were plotted against the DBH of the target trees. Linear regression was then used to describe the relationship between DBH and expanded occupancy area. These procedures were conducted using SAS 9.3 (SAS Institute, Cary, N.C.).

3.2.2 Estimation of Canopy Area from Expanded Occupancy

After calculating the mean expanded occupancy area for each polygon, the values were used to estimate tree canopy area. Under the assumption that expanded occupancy polygons were circular, the radius of the circle for the mean expanded occupancy area was calculated. With spacing between trees assumed to be equal throughout the polygon, this radius is equal to the distance between neighbouring tree stems. Dividing this radius by two is used to represent the crown radii of both the target and boundary trees, assuming that the target and boundary trees have equal crown areas. The estimate of the average target tree crown radius is then used to estimate the average tree crown area for individual trees within the polygon. The mean tree crown radius and associated area represents the physical canopy area an individual tree requires to compete within a particular polygon. This area also represents the minimum threshold value

that determines whether a LiDAR gap is large enough to host a tree or is simply interstitial space, an area too small to host a tree. LiDAR gaps smaller than the threshold area should not be included in any volume reconciliation calculations. This value is also used as a Y-intercept value for the predictive models generated in Chapter 2.

3.2.3 Volume Reconciliation

To reconcile the volume lost to gaps for each AVI polygon, the vector CHMs from Chapter 2 were used to generate a list of gaps which were sorted in descending order by area (the *gap list)*. Using the gap lists, LiDAR gaps with areas smaller than the mean tree crown area were removed from the list. This was done to remove gaps considered to be interstitial spaces within the polygon and not capable of hosting merchantable trees. For the remaining LiDAR gaps, the power function models generated in Chapter 2 were used to estimate expanded gap area. For all expanded gaps larger than 400 m^2, the expanded gap area was set to equal the LiDAR gap area. This prevented the overestimation of expanded gap area as gaps larger than this size exceeded the range of values measured in the field to develop the models for estimating expanded gap size.

The expanded gap area divided by the mean expanded occupancy area, rounded down to the nearest whole number represents an estimate of the number of mature trees that could be inserted into each gap. The volume of a merchantable tree was estimated using provincial taper equations (Huang, 1994) and the mean DBH calculated in Section 3.2.1. Multiplying the number of trees lost to gaps by the estimated volume for each tree provides an estimate of lost volume for the polygon and an estimate of lost volume per hectare.

To determine whether this estimate of volume loss to gaps is reasonable, estimates of actual yield for each polygon are required. Estimates of actual polygon volume for the entire polygon and for the individual fragments came from temporary sample plots (TSPs) measured by Tansanu (2007). Estimates using TSPs across the entire polygon, weighted by fragment area, were considered to represent the average polygon volume. To estimate the volume of a fully stocked or near fully stocked polygon, the weighted volume from the TSPs in the canopy cover fragments classed as 8 were used in the two aspen polygons. With the highest canopy cover in the spruce polygon being classed as a 7, the TSPs in these fragments were used to estimate fully stocked volume in the spruce polygon.

Adding the volume per hectare lost to gaps to the average volume per hectare for the entire polygon provides an estimate of the potential volume per hectare for the polygon when no gaps are present. This number can then be compared to the fully stocked volume from the high canopy cover fragments within the polygon.

3.3 Results

3.3.1 Estimation of Expanded Occupancy

3.3.1.1 Aspen Data

For Polygon 6796103, 30 trees were selected using the systematic sampling grid. The mean DBH was 27.6 cm with values ranging from 21.2 cm to 34.2 cm. The mean expanded occupancy area surrounding each tree was 28.4 m^2 with values ranging from 3.5 m^2 to 84.0 m^2. Descriptive statistics for the DBH and occupancy area for this polygon are presented in Table 3.2. The linear model relating DBH to occupancy area is represented by the following equation:

$$Y = 38.041 - 0.348x \qquad (3.1)$$

where (Y) is the estimated occupancy area in m^2 and (x) is the DBH of the tree in cm. The relationship between DBH and expanded occupancy was not statistically significant (p = 0.697, R^2 = 0.006, RMSE = 16.80). A scatterplot of these results is presented in Figure 3.1.

For Polygon 6886289, 27 trees were selected using the systematic sampling grid. The mean DBH was 26.1 cm with values ranging from 19.9 cm to 34.7 cm. The mean expanded occupancy area was 27.7 m^2 with values ranging from 5.1 m^2 to 57.9 m^2. Descriptive statistics for the DBH and occupancy area for this polygon are presented in Table 3.1. The linear model relating DBH to occupancy area is represented by the following equation:

$$Y = -8.442 + 1.385x \qquad (3.2)$$

where (Y) is the estimated occupancy area in m^2 and (x) is the DBH of the tree in cm. The relationship between DBH and expanded occupancy area was statistically significant (p = 0.019, R^2 = 0.202, RMSE = 12.49). A scatterplot of these results is presented in Figure 3.2.

3.3.1.2 White Spruce Data

For Polygon 6566412, 29 trees were selected using the systematic sampling grid. The mean DBH was 22.1 cm with values ranging from 15.1 cm to 30.8 cm. The mean expanded occupancy area was 27.0 m^2 with values ranging from 4.3 m^2 to 66.5 m^2. Descriptive statistics for the DBH and occupancy area for this polygon are presented in Table 3.3. The linear model relating DBH to occupancy area is represented by the following equation:

$$Y = 15.854 + 0.505x \qquad (3.3)$$

where (Y) is the estimated occupancy area in m^2 and (x) is the DBH of the tree in cm. The relationship between DBH and expanded occupancy area was not statistically significant (p = 0.3927, R^2 = 0.0272, RMSE = 13.60). A scatterplot of these results is presented in Figure 3.3.

Table 3.1: Descriptive statistics (mean, variance, standard deviation and range) for DBH and expanded occupancy area data collected for Polygon 6796103 (n=30)

	DBH (cm)	Expanded Occupancy Area (m^2)
Mean	27.6	28.4
Variance	12.4	274.0
Standard Deviation	3.5	16.5
Minimum	21.2	3.5
Maximum	34.2	86.0

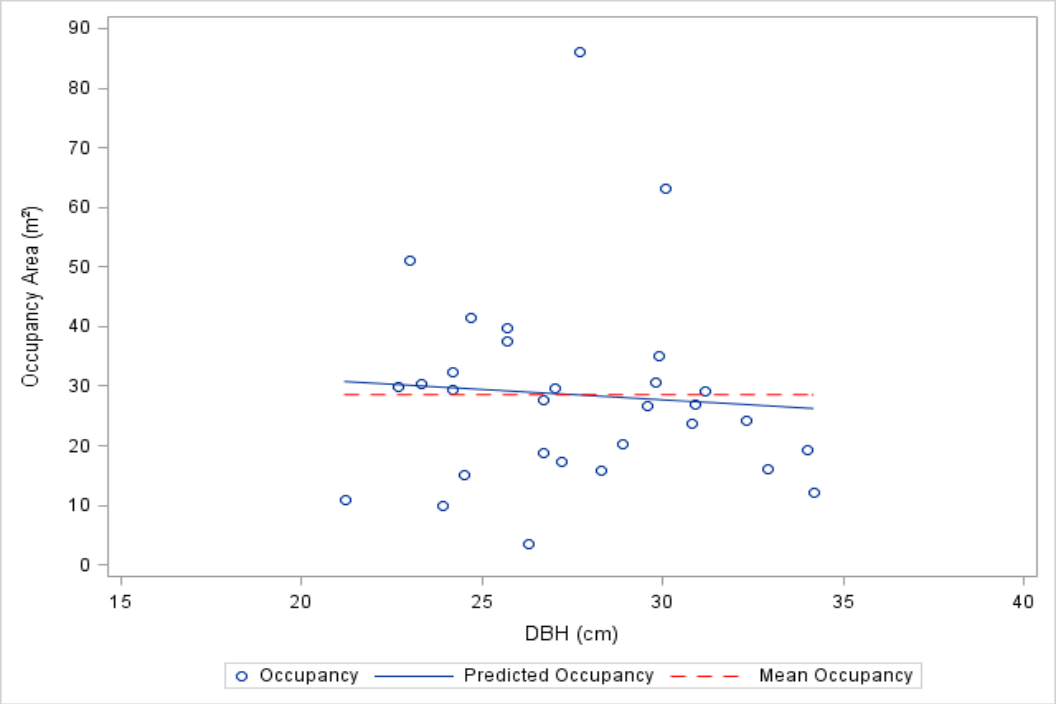

Figure 3.1: Plot of DBH against expanded occupancy area for Polygon 6796103 (n=30).

Table 3.2: Descriptive statistics (mean, variance standard deviation and range) for DBH and expanded occupancy area data collected for Polygon 6886289 (n=27)

	DBH (cm)	Expanded Occupancy Area (m^2)
Mean	26.1	27.7
Variance	19.8	188.1
Standard Deviation	4.45	13.7
Minimum	19.9	5.1
Maximum	34.7	57.9

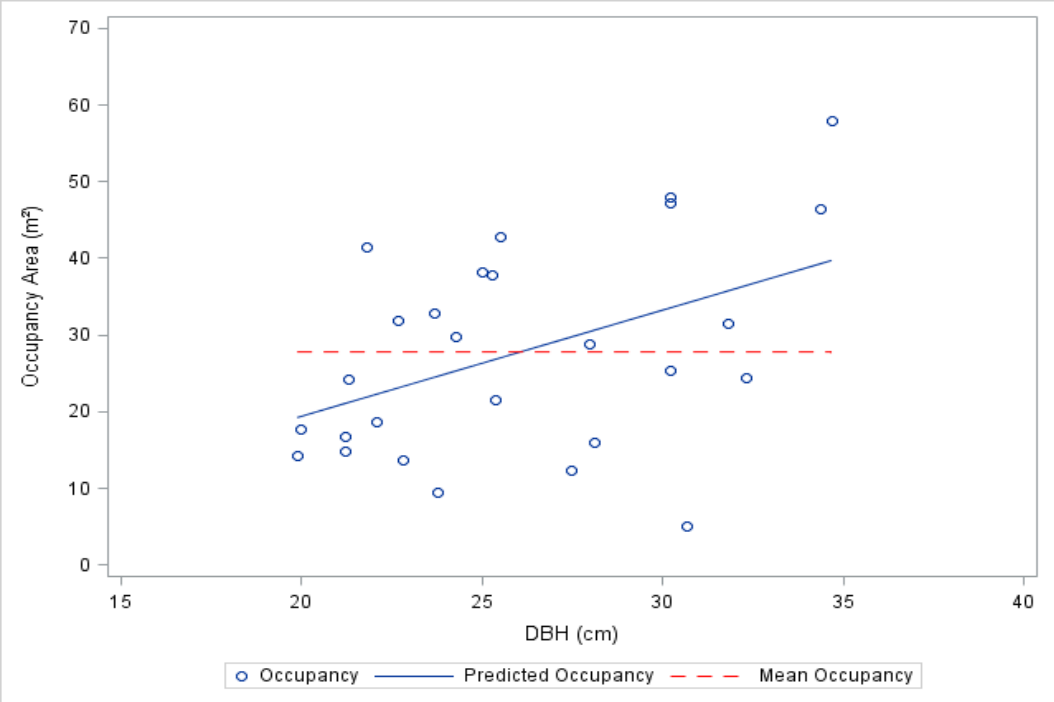

Figure 3.2: Plot of DBH against expanded occupancy area for Polygon 6886289 (n=27).

Table 3.3: Descriptive statistics (mean, variance, standard deviation and range) for DBH and expanded occupancy data collected for Polygon 6566412 (n=29).

	DBH (cm)	Expanded Occupancy Area (m^2)
Mean	22.1	27.0
Variance	19.5	183.4
Standard Deviation	4.4	13.5
Minimum	15.1	4.3
Maximum	30.8	66.3

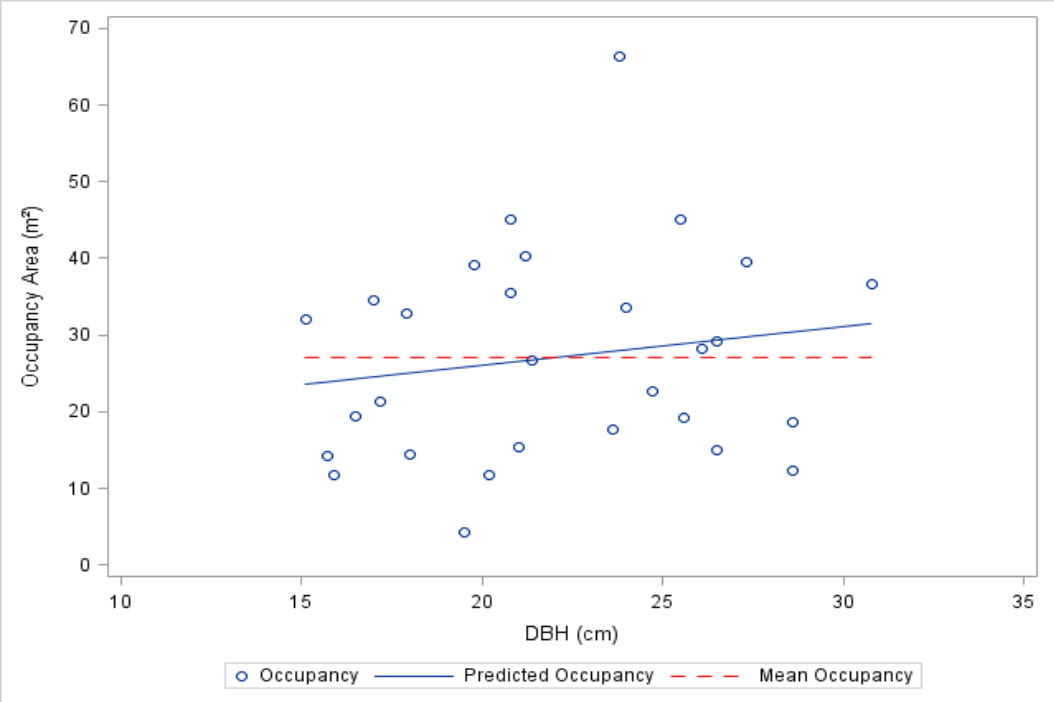

Figure 3.3: Plot of DBH against expanded occupancy area for Polygon 6566412 (n=29).

3.3.2 Estimating Average Tree Crown Area and Crown Radius

The average tree crown area for individual trees found in fully stocked fragments is an estimate of the crown area required by a single tree of the same size and species to be competitive within that stand. This area is estimated using the average expanded occupancy area by assuming crowns are circular and equally allocating crown to both the target tree and its neighbouring boundary trees. Table 3.4 shows expanded occupancy area and the associated occupancy radius for the three polygons and the estimates of crown area and radius that were obtained from these numbers. For Polygon 6796103, the average expanded occupancy area is 28.4 m^2. Assuming this area is circular, the expanded occupancy radius is 3.01 m. Dividing this occupancy radius equally between target trees and boundary trees gives a target tree crown radius of 1.5 m. The tree crown area of a circular crown with a radius of 1.5m is 7.1 m^2. In Polygon 6886289 tree crown area was estimated at 6.9 m^2, and in Polygon 6566412 tree crown area was estimated at 6.8 m^2. Since the crown area of these trees represents the minimum gap area that would be needed in the canopy to accommodate a mature tree, a LiDAR gap must be larger than this average tree crown area before it can be occupied by a merchantable tree. To ensure our assumptions were reasonable, we compared our crown radii to estimates calculated using a published crown radius formula (Stadt *et al*., 2005) and the mean DBH calculated for each polygon. Using Stadt *et al*.'s equations, the estimated crown radius for Polygon 6796103 was 2.4 m, Polygon 6886289 was estimated at 2.32 m, and Polygon 6566412 was estimated at 1.7 m (Data not shown). Our results indicate that our tree crown radii are smaller than those predicted by Stadt *et al*.

Table 3.4: Estimates of tree crown area and radius based on expanded occupancy area and radius calculated for the three research polygons analysed.

Polygon Number	Leading Species	Expanded Occupancy Area (m^2)	Expanded Occupancy Radius (m)	Tree Crown Radius (m)	Tree Crown Area (m^2)
6796103	Aspen	28.4	3.0	1.5	7.1
6886289	Aspen	27.7	3.0	1.5	6.9
6566412	White Spruce	27.0	2.9	1.5	6.8

3.3.3 Estimating Volume Lost to Canopy Gaps and Total Polygon Volume

3.3.3.1 Aspen Data

For Polygon 6796103, the total polygon area was 65.5 ha (Table 3.5). An anthropogenic disturbance (a well site) was removed from the calculations bringing the net polygon area to 63.1 ha. Using the vector CHM created in Chapter 2, the total LiDAR gap area was calculated to be 19.5 ha (30.9% of the total area). All LiDAR gap areas smaller than the crown areas presented in

Table 3.4 were removed as they were considered interstitial space as canopy gaps of this size would be too small to host a canopy tree. These gaps were removed from the gap list, leaving 18.3 ha of merchantable LiDAR gap area. Expanded gap area was estimated for the merchantable gaps using the non-linear model generated in Chapter 2 (Equation 2.4) that relates LiDAR gap area to expanded gap area. The estimate of total expanded gap area from the merchantable LiDAR gaps was 39.2 ha. For gaps larger than 400 m^2, expanded gap area was set to be equal to the LiDAR gap area to prevent overestimation of expanded gap area. For each merchantable gap, the expanded gap area was divided by mean expanded occupancy (28.4 m^2) and rounded down to the nearest whole number. This provides an estimate of 12881 trees lost to gaps. Rounding down to the nearest whole tree prevents the inclusion of partial trees within individual gaps and explains the discrepancy when the total expanded gap area (39.1 ha) is divided by the mean expanded occupancy (28.4 m^2) but does not equate to the expected 13762 trees. Multiplying the number of lost trees by the estimated volume per tree (0.6 m^3) results in an estimate of 7728.6 m^3 or 122.5 m^3/ha of lost volume within the polygon. Based on TSP volume estimates collected by Tansanu (2007), the average volume within the polygon is 301.4 m^3/ha. Adding the estimate of lost volume (122.5 m^3/ha) to Tansanu's estimate of average polygon volume (301.4 m^3/ha), we estimate a potential polygon volume of 423.9 m^3/ha. The average volume from TSPs found within the fragments of highest canopy cover within the polygon (classed as 8 or greater) was 358.6 m^3/ha. The difference between Tansanu's fully stocked polygon volume (358.6 m^3/ha) and the potential polygon volume (423.9 m^3/ha) is 69.6 m^3/ha. Considering the volume loss per hectare (122.5 m^3/ha) and estimated potential polygon volume (423.9 m^3/ha), the volume loss per hectare is estimated to be 28.9% for this polygon (Table 3.5).

For Polygon 6886289, the total polygon area was 27.6 ha. An anthropogenic disturbance (a cutline) was removed from the calculations bringing the net polygon area to 26.9 ha. Using the vector CHM created in Chapter 2, the total LiDAR gap area was calculated to be 2.9 ha. With gaps smaller than 6.9 m^2 being too small to host a canopy tree, they were removed from the gap list, leaving 2.8 ha of merchantable LiDAR gap area. Expanded gap area was estimated for the merchantable gaps using the non-linear model generated in Chapter 2 (Equation 2.6) that relates LiDAR gap area to expanded gap area. The estimate of total expanded gap area from the merchantable LiDAR gaps was 10.7 ha. For gaps larger than 400 m^2, expanded gap area was set to be equal to the LiDAR gap area to prevent overestimation of expanded gap area. For each merchantable gap, the expanded gap area was divided by mean expanded occupancy area (27.7 m^2) and rounded down to the nearest whole number. This provides an estimate of 3722 trees lost

to gaps. Rounding down to the nearest whole tree prevents the inclusion of partial trees and explains the discrepancy when the total expanded gap area (10.7 ha) is divided by the mean expanded occupancy area (27.7 m^2) but does not equate to the expected 3861 trees. Multiplying the number of lost trees by the estimated volume per tree (0.6 m^3) results in an estimate of 2233.2 m^3 or 83.1 m^3/ha of lost volume within the polygon. Based on TSP volume estimates collected by Tansanu (2007), the average volume within the polygon was 371.0 m^3/ha. Adding the estimate of lost volume (83.1 m^3/ha) to Tansanu's estimate of average polygon volume (371.0 m^3/ha) we estimate a potential polygon volume of 454.1 m^3/ha. The average volume from the TSPs found within the fragments of highest canopy cover (classed as 8 or greater) was 427.7 m^3/ha. The difference between Tansanu's fully stocked polygon volume (427.7 m^3/ha) and the potential polygon volume (454.1 m^3/ha) is 26.4 m^3/ha. Considering the volume loss per hectare (83.1m^3/ha) and the estimated potential polygon volume (454.1 m^3/ha), the volume loss per hectare is estimated to be 18.3% for this polygon. These results are presented in Table 3.6.

From these results, Polygon 6796103 has a relationship between merchantable LiDAR gap area (29.0%) and Volume Loss percentage (28.9%) of approximately 1:1. This shows that for every percentage point of polygon area classified as merchantable LiDAR gap there will be a loss of potential volume of just under 1%. For Polygon 6886289, the relationship between merchantable LiDAR gap area (10.2%) and Volume Loss percentage (18.3%) is 1:1.85. This shows that for every percentage point of polygon area classified as merchantable LiDAR gap there will be a loss of potential volume of 1.9%. These results are summarized in Table 3.6.

Table 3.5: Statistics for Polygons 6886289 and 6796103 relating to the reconciliation of LiDAR canopy height models to volume sampling data. Polygon 6796103 has had a 2.4 ha anthropogenic disturbance (well site) removed from all area calculations and Polygon 6886289 had a 0.68 ha anthropogenic disturbance (cutline) removed from all area calculations.

	Polygon 6796103	**Polygon 6886289**
Total Polygon Area	65.5	27.6
Total polygon Area with Anthropogenic disturbances removed	63.1 ha	26.9 ha
Total LiDAR Gap Area	19.5 ha	2.9 ha (10.9%)
Total LiDAR gap area estimate (merchantable gaps only)	18.3 ha	2.8 ha
Expanded gap area estimate (merchantable gaps only)	39.2 ha (62.1%)	10.7 ha (39.8%)
Mean Occupancy Area	28.4 m^2	27.7 m^2
Number of trees lost to gaps (Expanded gap area/Mean Occupancy Area)	12881 trees	3722 trees
Volume lost to gaps (Trees lost to Gaps *0.6 m^3; where 1 tree = 0.6 m^3)	7728.6 m^3	2233.2 m^3
Volume loss per hectare (Volume Lost to Gaps/Total Polygon Area)	122.5 m^3/ha	83.1 m^3/ha
Average Polygon Volume (TSP estimate)	301.4 m^3/ha	371.0 m^3/ha
Fully Stocked Polygon Volume (TSP estimates from fragments CC >=8)	358.6 m^3/ha	408.6 m^3/ha
Potential Polygon volume (Average Polygon Volume + Volume Loss per hectare)	423.9 m^3/ha	454.1 m^3/ha
Difference between Potential Polygon Volume and Fully Stocked Polygon Volume	65.3 m^3/ha	45.5 m^3/ha
Volume Loss Estimate (Volume Loss Per Hectare/Potential Polygon Volume)	28.9%	18.3%

Table 3.6: The relationships between LiDAR gap area percentage and volume loss percentage for aspen Polygons 6796103 (leaf off) and 6886289 (leaf on).

Polygon	**Merchantable LiDAR Gap Area Percentage (%)**	**Volume Loss Percentage (%)**	**LiDAR Gap Area % to Volume Loss % Ratio**
6796103	29.0	28.9%	1:1
6886289	10.2%	18.3%	1:1.85

3.3.3.2 White Spruce Data

For Polygon 6566412, the total polygon area was 12.9 ha (Table 3.7). An anthropogenic disturbance (a road) was removed from the calculations bringing the net polygon area to 11.7 ha. Using the vector CHM created in Chapter 2, the total LiDAR gap area was calculated to be 4.9 ha (41.7% of the total area). With LiDAR gaps smaller than 6.8 m^2 being too small to host a canopy tree, these gaps were removed from the gap list, leaving 4.7 ha of merchantable LiDAR gap area. Expanded gap area was estimated for the merchantable gaps using the non-linear model generated in Chapter 2 (Equation 2.8) that relates LiDAR gap area to expanded gap area. The estimate of total expanded gap area was 5.9 ha. For gaps larger than 400 m^2, expanded gap area was set to be equal to the LiDAR gap area to prevent overestimation of expanded gap area. Additionally, when the model predicted expanded gap area to be smaller than the LiDAR gap area, the expanded gap area was set to be equal to the LiDAR gap area. For each merchantable gap, the expanded gap area was divided by mean expanded occupancy (27.0 m^2) and rounded down to the nearest whole number. This provides an estimate of 1985 trees lost to gaps. Rounding down to the nearest whole tree prevents the inclusion of partial trees and explains the discrepancy when total expanded gap area (5.9 ha) is divided by expanded occupancy area (27.0 m^2), but does not equal the expected 2196 trees. Multiplying the number of lost trees by the estimated volume per tree (0.3 m^3) results in an estimate of 595.5 m^3 or 51.1 m^3/ha of lost volume within the polygon. Based on TSP volume estimates collected by Tansanu (2007) the average volume within the polygon was 227.9 m^3/ha. Adding the estimate of lost volume (51.1 m^3/ha) to Tansanu's estimate of average polygon volume (227.9 m^3/ha) we estimate a potential polygon volume of 279.0 m^3/ha. The average volume from the TSPs found within the fragments of highest canopy cover (classed as 7) was 230.8 m^3/ha. The difference between Tansanu's fully stocked polygon volume (230.8 m^3/ha) and the potential polygon volume (279.0 m^3/ha) was 48.2 m^3/ha. Considering the volume loss per hectare (51.1 m^3/ha) and the estimated potential polygon volume (279.0 m^3/ha), the volume loss per hectare is estimated to be 18.3% for the polygon. These results are presented in Table 3.7.

From these results, Polygon 6566412 has a relationship between merchantable LiDAR gap area (40.0%) and Volume loss percentage (15.0%) of 1:0.45. This shows that for every percentage point of area classified as merchantable LiDAR gap, there will be a loss of 0.5% potential volume. These results are summarized in Table 3.8.

Table 3.7: Statistics for Polygon 6566412 relating to the reconciliation of LiDAR canopy height model to volume sampling data. A 1.2 ha area anthropogenic disturbance (road) was removed from all area calculations.

	Polygon 6566412
Total polygon Area	12.9 ha
Total polygon Area with Anthropogenic disturbances removed	11.7 ha
Total LiDAR gap area estimate	4.9 ha
Merchantable LiDAR gap Area	4.7 ha
Expanded gap area estimate (merchantable gaps only)	5.9 ha
Mean Occupancy Area	27.0 m2
Number of trees lost to gaps (Expanded gap area/Mean Occupancy Area)	1985 trees
Volume lost to gaps (Trees lost to Gaps *0.3; where1 tree = 0.3 m3)	595.5 m3
Volume loss per hectare (Trees Lost to Gaps/Total Polygon Area)	51.1 m3/ha
Average Polygon Volume (TSP estimate)	227.9 m3/ha
Fully Stocked Polygon Volume (TSP estimate from stands with CC =7)	230.8 m3/ha
Potential Polygon volume (Average Polygon Volume + Volume Loss per hectare)	279.0 m3/ha
Difference between Fully Stocked Polygon Volume and Potential Polygon Volume	48.2 m3/ha
Volume loss Estimate (Volume Loss Per Hectare/Potential Polygon Volume)	18.3%

Table 3.8: The relationship between LiDAR gap area percentage and Volume Loss percentage for Polygon 6566412.

Polygon	Merchantable LiDAR Gap Area Percentage	Volume Loss Percentage	Merchantable LiDAR Gap Area % :Volume Loss % Ratio
6566412	40.0	18.3	1:0.45

3.4 Discussion

3.4.1 Expanded Occupancy Determination

The results from the individual tree occupancy sampling show that within the fully stocked areas of a polygon, the expanded occupancy area of the canopy trees has a weak relationship with tree DBH (R^2 values of 0.006, 0.202 and 0.027). Since one would expect crown size to increase with DBH (Stadt *et al*., 2005), it is reasonable to expect that expanded occupancy areas would also increase accordingly. However, the lack of statistical significance in these

relationships suggests that although DBH and crown area are correlated, the expanded occupancy area of canopy trees in fully stocked areas is quite variable. This lack of significance may be attributed to the relatively narrow range of DBHs sampled. In this study, we focused on a specific population of trees within each polygon: canopy trees within fully stocked areas that had fully enclosed crowns. Our population is similar to a mature vigorous stand that shows little variability in expanded gap spatial structure but may show variability in DBH. To contrast this, mature aspen stands undergoing breakup may have several cohorts of trees of different sizes, ages and social classes in close proximity. Their size, DBH, height and crown areas could all have been influenced by stand density, tree position in the canopy, current and past competition, and other factors (Sattler et al., 2012). With Pretszch (2014) showing that trees can adjust crown length without adjusting crown width, this suggests that a vigorous tree does not need to have large occupancy areas. A random sample balanced over all sizes and ages would likely have a wider range of DBHs and expanded gap sizes which would have likely resulted in stronger relationships.

Beyond sample size, there may also be biological reasons for the lack of a relationship. As stands develop, mortality of individual trees and the ensuing crown encroachment of the remaining canopy trees should allow the occupancy areas to increase in size. However, in cases of high stocking, crown sizes will be smaller and crown shyness is likely a major factor that prevents individual tree crowns from growing larger than those of neighbouring trees (Long and Smith, 1992), keeping the occupancy areas small. Interestingly, the average expanded occupancy area was not very different over the three polygons. The two aspen polygons have approximately the same age and average DBH (Tansanu, 2007), so it appears that average occupancy area may be quite stable, relative to DBH. The spruce polygon had a smaller DBH, but the expanded occupancy area was similar to aspen. Crown size and other characteristics are species specific (Stadt *et al*., 2005) therefore one would expect occupancy to be species specific. While our polygons were primarily mature, pure polygons; a polygon with a mixture of species will likely add an additional factor to measuring occupancy (Pretzsch, 2014). Full stocking at different ages may also result in different occupancy areas due to changes in tree and crown sizes. Although the primary use of an occupancy measurement would be in estimating volume loss at rotation age, more research to further explore how expanded occupancy changes by species, species mixture and age is needed and would support development of dynamic models.

In the three polygons measured, the precision of the expanded occupancy measurements may have been limited by the precision of the GPS unit used to record boundary tree locations. The minimum expanded occupancy measurements in all three cases appeared lower than

expected, although there is little literature pertaining to aspen and white spruce occupancy. We used a mapping grade GPS (Trimble GeoXT 6000) that had a maximum precision of approximately 0.5 meters. We do not believe this was achieved even with a collection of 50 hits per tree location. Collecting fifty hits is the Alberta Environment and Sustainable Resource Development standard for recording corners in PSPs (Cosmin Tansanu, Personal Communication, 2014). The accuracy of the area estimates was probably much higher in the aspen stands than the spruce polygons as there was no foliage to impede the GPS. This was not the case for the spruce polygon and in some cases it was difficult to obtain the desired hits. We assume however that GPS errors are random and there would be no systematic bias to them. We did not validate locations but expected individual point locations to be within one or two meters of the true location. More work into the accuracy and precision of GPS units in forest conditions is needed.

3.4.2 Tree crown radius measurements

Tree crown radii were estimated from expanded occupancy under the assumption that crowns were circular and equidistant with bordering trees. The assumption of circular crowns is mathematically and computationally convenient, accepting that crowns can be quite variable in size and shape for different species (Stadt *et al*., 2005). The overall implications of these assumptions were not explored but may be a topic of future study. The use of LiDAR or high resolution photography to measure crowns may be an avenue to explore, providing that high resolution LiDAR scans or photography are available (Gaulton and Malthus, 2010). To ensure that our crown area estimates were realistic, we compared our crown radii to calculated estimate of tree crown radii using DBH to crown area relationships developed by Stadt *et al*. (2005). The estimates of crown radii based on expanded occupancy were slightly smaller than those calculated using Stadt *et al*.'s equations. This is likely because estimates based on expanded occupancy were biased towards trees that had full crown enclosure. Comparatively, the trees used by Stadt *et al*. to develop the DBH to crown radius formula came from a range if canopy cover classes stored in a large database of randomly selected trees.

3.4.3 Estimating Gap Area

Using the tree crown area estimates, the results show that the majority of gaps within a polygon can be considered too small to support canopy trees. These gaps are referred to as interstitial space. Despite there being a large number of these gaps, the total area of these gaps is only a small proportion of the total polygon area and has little effect on the volume lost to gaps

within a polygon. For example, in Polygon 6796103 there were 1917 gaps classed as interstitial space. The total area of these interstitial spaces was 1.2 hectares, 1.6% of the total polygon area. Comparatively, the number of larger, merchantable gaps is a smaller proportion (n=1772 for Polygon 6796103) of the overall gap percentage, but affects potential polygon volume by 28% in that polygon. All gaps larger than 400 m^2 were considered to have expanded gaps equal to their LiDAR gaps. This was done because the expanded gap area estimates based on LiDAR area (Equations 2.4, 2.6, 2.8 and 2.10) developed in Chapter 2 did not include many gaps in the sample that were larger than 400 m^2. Additionally, the influence of crown overhang on expanded gap area should theoretically get smaller as gaps get larger. These equations, due to a lack of data did not reflect this effect such that expanded gaps became unrealistically large.

The process of removing small gaps was a critical step in estimating whether a gap was large enough to support a canopy tree. Since the raster resolution for differentiating gap versus canopy was 3 m x 3 m (9 m^2), a single pixel would be simplified to a size of approximately 5.8 m^2 in the vector model, with some variation depending on the arrangement of the pixels in the raster model. With these gaps being smaller than the estimated crown size for the polygon they could be removed from the gap list. There is a poor fit of the equation due to limited sampling. With small gaps not being sampled, the behaviour of the model was unreliable in this region. We also believe that sampling these small gaps increased the possibility of false negatives, especially with the low LiDAR hit count of 1.6 hits per m^2. When visiting these small gaps in the field we felt that in many cases these gaps were interstitial spaces.

The summation of all expanded gaps into one large gap area and then determining how many trees would fit into that area would also artificially inflate the total estimate of trees that would be lost to gaps. To account for this, the process of filling gaps with trees was done at the individual gap level. By ensuring that gaps would only be able to hold whole trees, fractional areas were dropped from these estimates. We also assumed that trees were of similar size over the polygon, and that the spacing between trees was at high densities. Although this is not always true, it was considered a reasonable approach for distributing trees within the gap areas.

To estimate the merchantable area lost to gaps from the LiDAR gaps, the use of expanded gaps was important. In situations where data sets may have a mixture of both leaf on and leaf off LiDAR scans for deciduous polygons, the amount of gap area will vary with the season. For example, if a single polygon was scanned in both leaf on and leaf off stages, the amount of gap area sensed during the leaf off stage would be greater than the amount seen in the summer. Without using the models developed in Chapter 2 to estimate expanded gap area, LiDAR gaps could be used, but they would not account for the true stand conditions, nor address differences

between leaf on and leaf off conditions. However, using LiDAR gaps would provide conservative estimates of gap area. This would also result in fewer gaps being considered merchantable. In estimating expanded gap area, the gap area on the ground is considered, instead of the opening in the canopy sensed by the LiDAR. This ensures that gaps with ground area to support canopy trees are not overlooked.

3.4.4 Reconciling Volume Lost To Gaps

The addition of the volume lost to gaps to the average stand volume taken from TSP measurements estimates the potential stand volume, the volume attained if all gaps were occupied by trees. These potential volume estimates were compared to actual stand estimates taken in the areas of high stocking within each polygon. The process of adding the volume lost to gaps to the average volume from the entire polygon was an attempt to reconcile whether the estimates of volume lost were reasonable. In all cases, these potential volumes were larger than the average volumes taken from the fully stocked areas in the polygon. This is not unexpected as the mean volume for the polygon included fully stocked volumes. Additionally, even in areas of high stocking some gaps still exist and the process of filling gaps with trees would have included filling those gaps that exist in the fully stocked potions of the polygon with trees. Overall, the process of reconciling volume using the TSPs, does demonstrate that estimates of potential stand volume obtained using the expanded gap methodology provides reasonable results.

Looking at the different percentages of gap loss between polygons we can see that while gaps are common in all polygons, local conditions and the nature of individual gaps can have different effects on volume loss for a polygon. In Chapter 4 we investigate the nature of individual gaps by linking them spatially to wet areas and predicting how this may affect our volume predictions.

3.4.5 Applications

The ability to discern between merchantable canopy gaps and interstitial spaces between trees has the potential to improve long term forest planning by accounting for gaps in growth and yield models. With many models using PSP data to develop growth curves, these models will show similar volume overestimation to that seen by Eriksson (1964), unless gaps are accounted for. Examples of programs that have the potential to account for volume loss due to gaps include Table Interpolation Program for Stand Yields (TIPSY) (B.C. Ministry of Forests, Lands and

Natural Resource Operations 2013) and the Mixedwood Growth Model (MGM) (Bokalo *et al.*, 2014).

To account for gaps in TIPSY, this model includes two operational adjustment factors (OAF1 and OAF2) as model parameters. These parameters adjust yield projections by considering gap presence as it models stand growth. The OAF1 parameter is an adjustment that is incorporated across the model to account for stocking gaps which are present throughout the life of a stand (B.C. Ministry of Forests, 1998[a]). The OAF2 parameter is a value which increases as the stand ages. This adjustment is used to account for the increased occurrence of gaps in a stand as a forest ages and trees die. The starting values and rate of increase for OAF2 are often held constant, however the OAF1 values can vary by stand and sampling can be used to determine how gaps affect individual stand types. Prior to the development of these LiDAR methods, random sampling was recommended as a method to estimate the value of OAF1 (B.C. Ministry of Forests, 1998[b]). With there being some difficulty in determining merchantable gaps from interstitial space in the field, the use of LiDAR has the potential to provide a more objective estimate of gap percentages and greatly reduce sampling efforts. To account for gaps in MGM, a gap loss percentage parameter is included in the model. Similar to OAF1, the gap loss percentage is a calculation of the percentage of stocking gaps that will be included in the model. The inclusion of this parameter reduces the growing area of the polygon, which increases competition between trees in the occupied portion of the polygon. This increase in competition reduces the overestimation of volume at the polygon level and will bring estimates closer to those expected.

For models that do not have a gap loss percentage or operational adjustment factor included in the model parameters other methods can be used so that gap percentages can be incorporated into model projections. One method would be to reduce polygon volume by the expected gap area prior to running the model. This would allow models to run in a similar way to models that do have gap loss parameters. Another way to adjust yields would be through a yield adjustment after the models have been run. By determining the rate at which volume decreases when gap area increases, a post-hoc adjustment can be done to projections to bring them closer to expected values.

Beyond forest planning, these methods can also be useful in forest operations. When forest polygons are harvested, average yields for a stratum may be used to estimate how much volume is available in an individual polygon. By estimating the amount of gaps from a recent LiDAR scan, it is possible to compare polygon conditions to the stratum averages and determine if gaps are more or less prevalent. By estimating how much volume may be harvested, it can

assist mill operators in ensuring they are harvesting sufficient stock. This can help ensure that the mill will not experience any shortages when harvesting is not occurring.

Outside of volume adjustments, these gap analysis methods also have the potential to be used in other forestry applications. For biodiversity studies that focus on forest gaps (e.g. De Grandpre *et al*., 2011), these methods can now allow for accurate identification of gaps which may be of interest before visiting a field site and for modelling ecosystem services associated with gaps. This could include gaps of particular sizes or shapes, or gaps with other characteristics that may be of interest. These methods can greatly reduce time in the field required to find appropriate sites.

3.5 Conclusions

This chapter has provided a methodology that uses individual canopy gap areas determined using LiDAR, and estimates of individual tree expanded occupancy to estimate how canopy gaps affect estimates of stand volume. By adding the estimates of volume loss to stand level volume estimates we get volume estimates that correspond well with volume measured in the areas of highest stocking. Through a variety of methods, adjustments can be made to account for gap area before growth is modelled, or post-hoc adjustments can be made based on the relationship of gap area to volume loss. These adjustments have the potential to improve long term planning by providing better estimates of growth potential. Further improvements that can further stratify gaps as temporary or persistent may improve these methods further.

References

Alberta Land and Forest Service. 1994. Permanent sample plot field procedures manual. Alberta Land and Forest Service, Forest Management Division, Forest Measurement Section. Edmonton, Alberta.

B.C. Ministry of Forests. 1998[a]. OAF1 Project Report #1. An overview of stocking gaps and OAF1 estimates for TIPSY. B.C. Ministry of Forests, Forest Practices Branch. Victoria, B.C.

B.C. Ministry of Forests. 1998[b]. OAF1Project Report #2. Ground-based survey method. B.C. Ministry of Forests, Forest Practices Branch. Victoria, B.C.

B.C. Ministry of Forests, Lands and Natural Resource Operations. A Table Interpolation Program for Stand Yields (TIPSY), Version 4.3. Ministry of Forests, Lands and Natural Resource Operations, Forest Analysis and Inventory Branch, Victoria B.C, Canada. **2013**. Available online: http://www.for.gov.bc.ca/hre/software/download.htm (accessed on 30 December 2014).

Bokalo, M.; Stadt, K.J.; Comeau, P.G.; Titus, S.J. Mixedwood Growth Model (MGM) (version MGM2010.xls). University of Alberta, Edmonton, Alberta, Canada. **2010**. Available online: http://www.rr.ualberta.ca/Research/MixedwoodGrowthModel.aspx (accessed on 20 November 2014).

Cumming, S.G., Schmiegelow, F.K., and Burton, P.J. 2000. Gap dynamics in boreal aspen stands: is the forest older than we think? Ecological Applications **10(3):** 744–759. doi: 10.2307/2641042

De Grandpre, L., Boucher, D., Bergeron, Y. and Gagnon, D. 2011. Effects of small canopy gaps on boreal mixedwood understory vegetation dynamics. Community Ecology **12(1):** 67 – 77. doi: 10.1556/ComEc.12.2011.1.9

Eriksson, H. 1962. A comparison between the yield figures for permanent sample plots and those for the stand as a whole. Royal College of Forestry, Department of Forest Yield and Research. Research Notes Nr:14. 72 pp. Printed in Swedish with English summary.

Gaulton, R., and Malthus, T.J. 2010. LiDAR mapping of canopy gaps in continuous cover forests: A comparison of canopy height model and point cloud based techniques. International Journal of Remote Sensing **31(5):** 1193 – 1211. doi: 10.1080/01431160903380565

Huang, S. 1994. Report #1: Individual tree volume estimation for Alberta: Methods of formulation and statistical foundations. Alberta Environmental Protection, Land and Forest Service, Forest Management Division.

Long, J.N. and Smith, F.W. 1992. Volume increment in *Pinus contorta* var. *latifolia*: the influence of stand development and crown dynamics. Forest Ecology and Management **53(1-4):** 53-64. doi: 10.1016/0378-1127(92)90033-6

MacIsaac, D., Comeau, P., and Macdonald, S.E. 2006. Dynamics of regeneration gaps following harvest of aspen stands. Canadian Journal of Forest Research **36(7):** 1818 – 1833. doi: 10.1139/X06-077

Pretzsch, H. 2014. Canopy space filling and tree crown morphology in mixed-species stands compared with monocultures. Forest Ecology and Management **327:** 251 – 264. doi: 10.1016/j/foreco.2014.04.027

Runkle, J.R. 1982. Patterns of disturbance in some old-growth mesic forests of eastern North America. Ecology **63(5)**: 1533–1546. doi: 10.2307/1938878

Sattler, D.F., Comeau, P.G., and Achim, A. 2014. Branch models for white spruce (*Picea glauca* (Moench) Voss) in naturally regenerated stands. Forest Ecology and Management **325:** 74 – 89. doi: 10.1016/j.foreco.2014.03.051

Stadt, K.J., Lieffers, V.J., Hall, R.J. and Messier, C. 2005. Spatially explicit modelling of PAR transmission and growth of *Picea glauca* and *Abies balsamea* in the boreal forests of Alberta and Quebec. Canadian Journal of Forest Research **35(1):** 1 – 12. doi: 10.1139/X04-141

Tansanu, C.S. 2007. The Role of Forest Stand Structure in Predicting Yield. M.Sc Thesis. University of Alberta. 129 pp.

Chapter 4: The Relationship between Canopy Gaps and Depth to Water Index

4.1 Introduction

Gaps are common in boreal forests and influence forest regeneration (MacIssac *et al*., 2006), stand structure (Cumming *et al*., 2000), and biodiversity (Bouget and Duelli, 2004; Chavez and Macdonald, 2010). Few studies have examined the effect of gaps on yield due to difficulties in enumerating the full population of gaps; however the development of LiDAR and other remote sensing techniques provides effective tools for quantifying the size and extent of gaps. In Chapter 2, methods were developed that enabled the determination of the dimensions and spatial distribution of gaps using LiDAR and GIS analysis. Other characteristics recommended by Runkle (1992) that could be assessed to characterize gaps include: gap microhabitat, gap age, adjacent forest type, gap aperture size, vegetation within the gap, gap site characterization (slope, aspect, elevation, soil conditions, topographic position), and the number of trees that died to form the gap (number of gap makers).

A population of gaps from a polygon will show common characteristics based on the characteristics of that polygon, for example, soil type, depth to water or tree species. Gaps will also display characteristics that are common between polygons. For example the different gap characteristics suggested by Runkle (1992) may be spatially arranged based on local land features such as contours, aspect, slope, hydrology, differences in overstory and understory vegetation, and soil characteristics. The temporal nature and dynamics of gaps may also link gap characteristics to the time since gap birth or how and when gap death is achieved, either through the expansion of tree crowns or from ingress of regeneration. Having additional information about the individual gaps, the polygon and landscape may permit researchers make better inferences about the nature of gaps and their influence as it related to their research questions.

The wet areas mapping (WAM) process, developed by Murphy *et al.* (2011), is a classification system that uses topographic data derived from the LiDAR point cloud to map stream flow channels and delineate soil drainage patterns at high resolution (White *et al*., 2012). Among the products created by the WAM process, maps of the depth to water (DTW) index are potentially useful in classifying gaps caused by high water tables or seasonal flooding. Depth to water approximates the elevation difference between the soil surface and the nearest open water features (such as flow channels and water pools), and provides an estimate of the degree of soil saturation based on the distance from any point of interest to these features (Murphy et al, 2011).

By combining CHMs developed in Chapter 2 with the DTW index, a stratification of canopy gaps based on the DTW drainage class is possible. This allows for the classification of gaps beyond simple presence and absence and identifies gaps whose presence may be caused by excessive ground water. In addition, mean gap size within each drainage class can be estimated. With the presence of open water being one cause of open forest canopies, such as in boreal fens, knowing whether large gaps are present only in these areas, or if gaps have similar sizes and frequencies in drier areas may also be of interest.

In this chapter the relationship between gaps measured in four polygons (as described in Chapter 2) and depth to water is examined using soil drainage classes that are estimated from the WAM estimates of depth to water. In particular, the relationship between soil drainage and the number and average size of gaps will be examined.

4.2 Methods

To analyse the relationship between canopy cover and the forest hydrology, raster models of the cartographic depth to water (DTW) index were acquired from Alberta Environment and Sustainable Resource Development (AESRD). The WAM rasters were created using algorithms in use during October of 2011. Each DTW raster was built using a 4 ha catchment area and has a pixel size of 1 m^2. In addition to the DTW rasters, the 3 m × 3 m raster versions of the canopy height models (CHMs) developed in Chapter 2 were also used in this analysis.

With a primary goal of identifying gaps which may have been caused by or influenced by high ground water, the CHMs were modified in ArcGIS 10.1 (Redlands, California) to remove anthropogenic disturbances and interstitial space from the models. Anthropogenic disturbances were removed because the creation of these gaps in the canopy is often accompanied by an alteration to the local drainage patterns. The inclusion of these gaps in the analysis would likely bias our analysis towards finding gaps in well drained areas. These disturbances were removed from each polygon CHM according to the boundaries provided during the photo interpretation of each polygon (Tansanu, 2007) using the "Erase" tool. In addition to removing anthropogenic disturbances, gaps classed as interstitial spaces were also removed using the average tree crown size found in each polygon. Interstitial spaces are ubiquitous, temporary gaps in the canopy with their presence not dictated by the presence of ground water. The inclusion of these gaps in the analysis would likely reduce the ability to predict gaps caused by high ground water because there is a disproportionate amount of dry area to wet area in each polygon. This has the potential to bias results towards finding gaps more frequently in dry areas. To remove interstitial space

from the CHM, several tools in the spatial analyst toolbox in ArcGIS 10.1 were used. The first step was to group pixels associated with continuous tracts of gap or canopy using the "Region Group" tool, grouping pixels using four neighbours. Following this, the groups of pixels with counts greater than one were extracted using the "Extract by Attributes" tool to create a mask layer of the gaps which were large enough to host one or more merchantable trees. By using this mask layer and the "Nibble" tool, the pixels that were not part of the mask were reclassified to match the classification of the pixels surrounding it. Using these processes, the resulting CHM for each polygon has no gaps caused by anthropogenic disturbance or interstitial space. It is noted that the gap areas calculated using this direct raster processing method are slightly different than those calculated in Chapter 2 and 3 using vector CHMs.

Each of these modified CHMs was then combined with the DTW raster using the "Combine" tool. This resulted in a new raster layer being created with unique pixel values based on the combination of canopy classification (1 for gap or 2 for canopy), and the depth to water index (in cm). With resolutions between the two rasters being different, the combine process created a raster at a 3 m^2 resolution. From this raster, counts of pixels based on their canopy classification and DTW value were then tabulated for each polygon. This was done using drainage classes defined by White *et al.* (2012), with the classes being: Very Poor (DTW < 10 cm); Poor (10 cm < DTW < 25 cm); Imperfect (25 cm < DTW < 50 cm); Moderately Well (50 cm < DTW < 100 cm); Well (100 cm < DTW < 2000 cm); and Exceedingly Well (DTW > 2000 cm). Additionally, the minimum DTW value was used to assign a DTW class for each gap occurrence. For each drainage class, the number of gaps per hectare and the mean gap size was tabulated based on this classification. For each gap, the minimum DTW value was used to classify the gap within a drainage class. This was done as gaps caused by wet areas are thought to be centered on areas with wetter soils and be bordered by better drained soils. For gaps classified within each drainage class, the mean gap area was also calculated. With some gaps having small areas around their centroids of poorly drained soils and these centroids being surrounded by better drained soils, there was potential for large mean gap areas in drainage classes with small total areas.

4.3 Results

4.3.1 Area Analysis

After combining the CHM raster and DTW raster, the pixel counts within each drainage class were tabulated and converted to areas in hectares (Table 4.1). For each polygon, the areas within each drainage class classified as gap or canopy area were also tabulated (Tables 4.2 and 4.3).

In the aspen polygons, Polygon 6796103 had 15.21 ha (23.36%) of area classified as very poor, poor, imperfect or moderately well and 49.90 ha (76.64%) of the area classified as well drained soils. Across the polygon approximately 32.6% of the area within each drainage class was classified as gap area. The gap area across the drainage classes ranged between 30.2% and 37.4% with the relative area decreasing slightly as the classes moved from the very poor to well drained soils. In Polygon 6886289, 1.77 ha (6.42%) of the area was classified as very poor, poor, imperfect and moderately well, and 25.67 (93.58%) was classified as well drained. When classified according to canopy cover, 12.9% of the area was classified as gap area with a high proportion of gap area in the very poor drainage class (39.3%). This proportion decreases as drainage improves to 11.7% in the well-drained soils.

In the spruce polygons, Polygon 6566412 had almost entirely (99.98%) well drained soils so no generalizations can be made about this polygon. Polygon 64106639 was found on a slope and therefore had a high proportion of both well drained (22.41 ha, 43.60%) and exceedingly well drained soils (27.27 ha, 53.05%) and only a small proportion of area that was considered very poor, poor, imperfect or moderately well drained (1.72 ha, 3.35%). When classified according to canopy cover, 28.0% of the area was classified as gap area with a high proportion of gaps in the very poor drainage class (52.2%). This proportion decreases as drainage improved to 26.3% in the exceedingly well drained soils.

Table 4.1: Area distributions amongst drainage classes for the four research polygons in this study. Areas attributed to anthropogenic disturbances and interstitial spaces are not included in this table.

	Aspen Polygons		Spruce Polygons	
Drainage Class	**Polygon 6796103 (ha)**	**Polygon 6886289 (ha)**	**Polygon 6566412 (ha)**	**Polygon 64106639 (ha)**
Very Poor (DTW<10 cm)	2.27 (3.49%)	0.28 (1.02%)	0	0.23 (0.45%)
Poor (10 cm<DTW<25 cm)	2.35 (3.89%)	0.26 (0.95%)	0	0.29 (0.56%)
Imperfect (25 cm<DTW<50 cm)	3.64 (5.59%)	0.36 (1.31%)	0	0.43 (0.84%)
Moderately Well (50 cm<DTW<100 cm)	6.95 (10.67%)	0.87 (3.17%)	0.01 (0.08%)	0.77 (1.50%)
Well (100 cm<DTW<2000 cm)	49.90 (76.64%)	25.67 (93.58%)	12.78 (99.98%)	22.41 (43.60%)
Exceedingly Well (DTW>2000 cm)	0	0	0	27.27 (53.05%)
Total Area	65.11	27.43	12.79	51.40

Table 4.2: Gap and canopy areas and percentages of area within each drainage class for the aspen polygons. Percentages indicate the percentage of areas in the drainage class that is gap or canopy. Areas attributed to anthropogenic disturbances and interstitial spaces are not included in this table.

	Polygon 6796103		Polygon 6886289	
Drainage Class	**Gap Area (ha)**	**Canopy Area (ha)**	**Gap Area (ha)**	**Canopy Area (ha)**
Very Poor (DTW<10 cm)	0.81 (35.7%)	1.46 (64.3%)	0.11 (39.3%)	0.17 (60.7%)
Poor (10 cm<DTW<25 cm)	0.88 (37.4%)	1.47 (62.6%)	0.10 (38.5%)	0.16 (61.5%)
Imperfect (25 cm<DTW<50 cm)	1.20 (33.0%)	2.44 (67.0%)	0.11 (30.6%)	0.25 (69.4%)
Moderately Well (50 cm<DTW<100 cm)	2.10 (30.2%)	4.85 (69.8%)	0.20 (23.0%)	0.67 (77.0%)
Well (100 cm<DTW<2000 cm)	16.21 (32.5%)	33.69 (67.5%)	3.01 (11.7%)	22.66 (88.3%)
Total Area	21.20 (32.6%)	43.91 (67.4%)	3.53 (12.9%)	23.90 (87.1%)

Table 4.3: Gap and canopy areas and percentages of area within each drainage class for the white spruce polygons. Percentages indicate the percentage of areas in the drainage class that is gap or canopy. Areas attributed to anthropogenic disturbances and interstitial spaces are not included in this table.

	Polygon 6566412		Polygon 64106639	
Drainage Class	**Gap Area (ha)**	**Canopy Area (ha)**	**Gap Area (ha)**	**Canopy Area (ha)**
Very Poor (DTW < 10 cm)	0 (0%)	0 (0%)	0.12 (52.2%)	0.11 (47.8%)
Poor (10 cm<DTW<25 cm)	0 (0%)	0 (0%)	0.11 (37.9%)	0.18 (62.1%)
Imperfect (25 cm<DTW<50 cm)	0 (0%)	0 (0%)	0.18 (41.9%)	0.25 (58.1%)
Moderately Well (50 cm<DTW<100 cm)	0.01 (100%)	0 (0%)	0.31 (40.3%)	0.46 (59.7%)
Well (100 cm<DTW<2000 cm)	5.90 (46.2%)	6.88 (53.8%)	6.48 (28.9%)	15.93 (71.1%)
Exceptionally Well (DTW>2000 cm)	0 (0%)	0 (0%)	7.18 (26.3%)	20.09 (73.7%)
Total Area	5.91 (46.2%)	6.88 (53.8%)	14.39 (28.0%)	37.01 (72.0%)

4.3.2 Gap Occurrences within drainage classes

To account for the unequal distribution of area within each drainage class, the number of gap occurrences within each drainage class was divided by the drainage class area to estimate the number of gaps per hectare (Tables, 4.4, 4.5, 4.6, and 4.7).

In the aspen polygons, Polygon 6796103 had the highest count of gap occurrences in well-drained soils, with 70.02% being found within this stratum. However, when calculated as gaps per hectare based on the area included in each drainage class, gaps are more prevalent in the very poorly drained soils (62.14 gaps/ha) and this prevalence decreased to 25.18 gaps/ha in the poor drainage class and further to 20.63 gaps/ha in the well-drained soil as drainage improved. The mean gap area was also larger in the very poor drained soils (426.45 m^2) and decreased as drainage improved. It should be noted that the mean gap area reflects the average area of gaps with a minimum DTW value and does not mathematically correlate to the total area in each DTW class. For Polygon 6886289, the highest count of gap occurrences was in the well-drained soils, with 89.61% of the gaps being found in this stratum. However, when calculated as gaps per hectare based on the area included in each drainage class, gaps are more prevalent in the very poorly drained soils (53.42 gaps/ha) and this prevalence decreased to 9.74 gaps/ha in the well-drained DTW class. The mean gap area was also larger in the very poor soils (649.29 m^2) and decreased to 73.72 m^2 as drainage improved.

In the spruce polygons, Polygon 64106639, approximately 94.44% of the gaps within the polygon were in either well drained or exceedingly well drained soils. As with the aspen polygons the prevalence of gaps per hectare in each drainage class was higher in the very poor soils (193.24 gaps/ha) and decreased to 24.64 gaps/ha in the exceedingly well drained soils. The trends in mean gap area for each stratum were also similar with larger gaps being found in very poor soils and mean gap size decreasing as drainage improved. Polygon 6566412 did not sufficient variation in soil drainage classes to be of much interest.

Table 4.4: Estimates of merchantable gaps per hectare and mean gap area for Polygon 6796103, an aspen polygon.

Drainage Class	Total Stratum Area (ha)	Gap Occurrences	Gaps/ha	Mean Gap Area[1] (m^2)
Very Poor (DTW < 10 cm)	2.27	141	62.14	426.45
Poor (10 cm<DTW<25 cm)	2.34	59	25.18	120.97
Imperfect (25 cm<DTW<50 cm)	3.64	90	24.74	134.20
Moderately Well (50 cm<DTW<100 cm)	6.95	151	21.73	134.52
Well (100 cm<DTW<2000 cm)	49.91	1030	20.63	109.02
Entire Polygon	65.10	1471	22.60	144.09

Table 4.5: Estimates of merchantable gaps per hectare and mean gap area for Polygon 6886289, an aspen polygon.

Drainage Class	Total Stratum Area (ha)	Gap Occurrences	Gaps/ha	Mean Gap Area[1] (m^2)
Very Poor (DTW < 10 cm)	0.28	14	53.42	649.29
Poor (10 cm<DTW<25 cm)	0.25	4	15.70	99.00
Imperfect (25 cm<DTW<50 cm)	0.36	1	2.76	144.00
Moderately Well (50 cm<DTW<100 cm)	0.87	10	11.52	330.30
Well (100 cm<DTW<2000 cm)	25.67	250	9.74	73.72
Entire Polygon	27.43	279	10.21	111.52

Table 4.6: Estimates of merchantable gaps per hectare and mean gap area for Polygon 6566412, a white spruce polygon.

Drainage Class	Total Stratum Area (ha)	Gap Occurrences	Gaps/ha	Mean Gap Area[1] (m^2)
Moderately Well (50 cm<DTW<100 cm)	0.01	1	100.00	8802.00
Well (100 cm<DTW<2000 cm)	12.78	267	20.89	149.93
Entire Polygon	12.79	268	20.96	182.22

[1] For each gap occurrence, the minimum DTW value was used to determine which drainage class it belonged to. Based on this classification mean gap area was calculated. Many gaps contained pixels from more than one drainage class, explaining the large mean gap areas.

Table 4.7: Estimates of merchantable gaps per hectare and mean gap area for Polygon 64106639, a white spruce polygon.

Drainage Class	Total Gap Area (ha)	Gap Occurrences	Gaps/ha	Mean Gap Area[1] (m^2)
Very Poor (DTW < 10 cm)	0.23	44	193.24	421.36
Poor (10 cm<DTW<25 cm)	0.29	8	27.95	217.13
Imperfect (25 cm<DTW<50 cm)	0.43	10	23.10	224.10
Moderately Well (50 cm<DTW<100 cm)	0.77	10	12.98	46.80
Well (100 cm<DTW<2000 cm)	22.41	551	24.58	114.83
Exceptionally Well (DTW>2000 cm)	27.27	672	24.64	85.75
Entire Polygon	51.40	1295	25.20	111.11

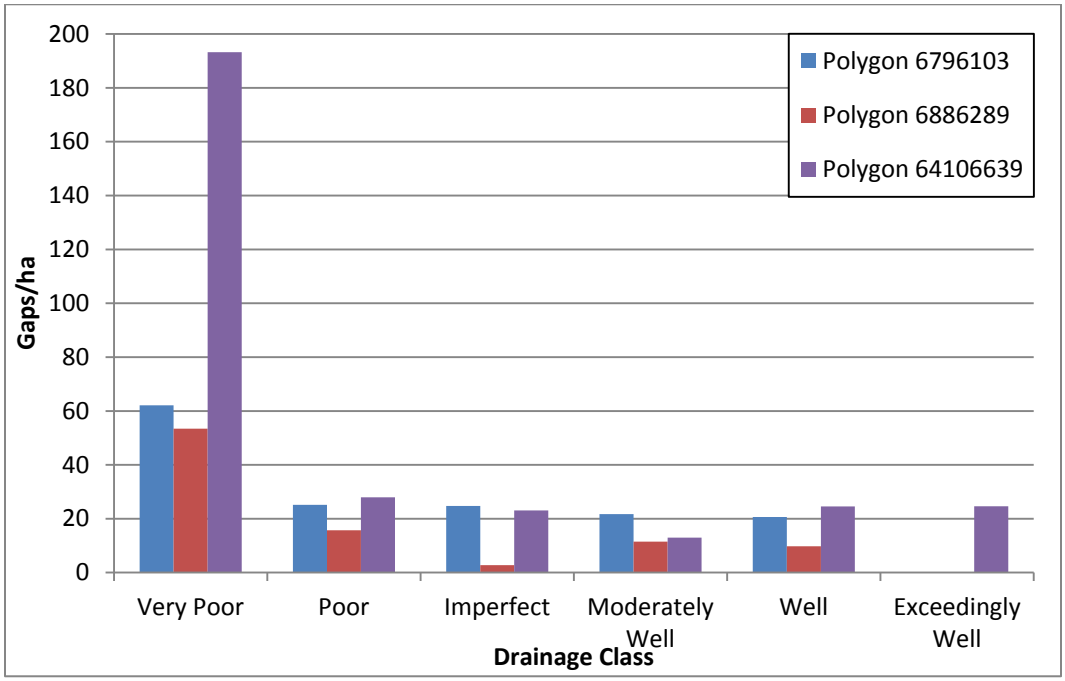

Figure 4.1: Estimates of gaps per hectare for each polygon stratified by drainage class.

[1] For each gap occurrence, the minimum DTW value was used to determine which drainage class it belonged to. Based on this classification mean gap area was calculated. Many gaps contained pixels from more than one drainage class, explaining the large mean gap areas.

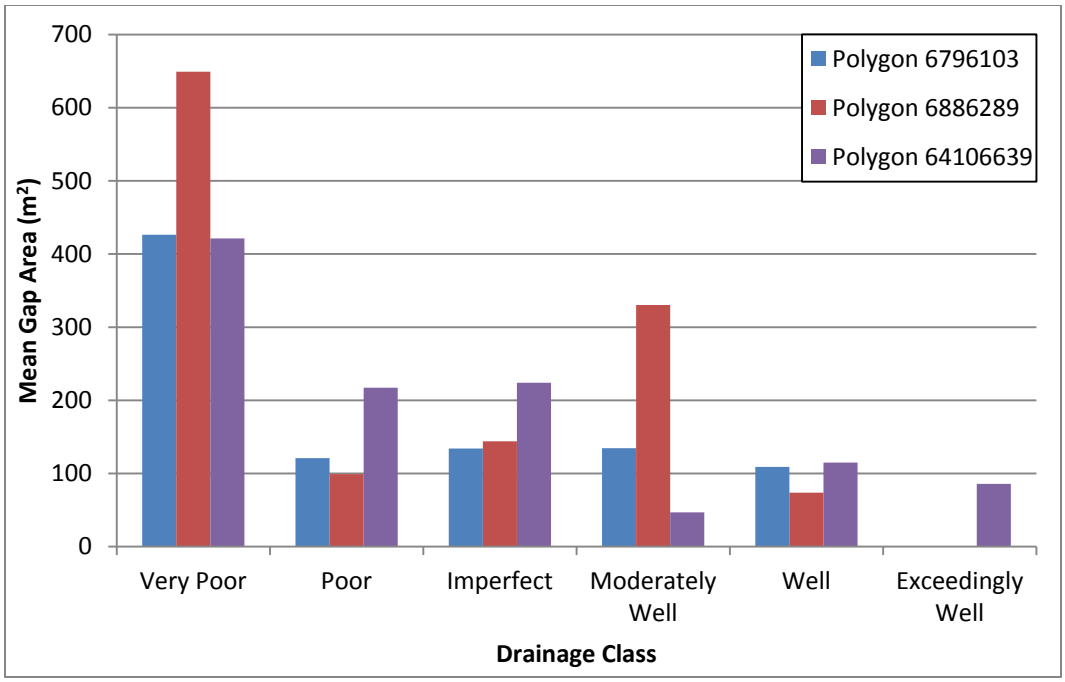

Figure 4.2: Estimates of mean gap area for each polygon stratified by drainage class.

4.4 Discussion

4.4.1 Area Analysis and Predictions of Gap Drainage

The results of the raster analysis show that Polygon 6566412, a white spruce polygon, had only a small proportion of the polygon area that was not well drained (approximately 81 m^2 classified as moderately well drained). The lack of diversity in drainage for this polygon prevents us from making any further inferences about the effects of forest hydrology on these gaps.

For polygons 6886289 (aspen) and 64106639 (white spruce), trends of higher canopy gap proportions in poorly drained soils and lower proportions of gaps in better drained soils are clearly evident. These results correspond to the observations by MacIssac *et al*. (2006) that gaps were more prevalent in wet areas. Polygon 6796103 (aspen) did not show this trend, and instead had a consistent proportion of approximately 32% gaps across all drainage classes. This exception to the trend seen in the other two polygons may be explained by the CHM used in the analysis. For this polygon, the LiDAR scan used was conducted during the leaf off period, while the other aspen polygon was leaf on, and the spruce polygon was not subject to seasonality. Using a scan during the leaf off period provides higher estimates of gap area than full foliage scans and as a result the proportion of merchantable gap area increases. With poorly drained areas already having a high proportion of gap pixels, the addition of any pixels due to seasonality should not change the proportion of gap pixels to canopy pixels to a large degree. However, in

better drained areas where canopy cover is notably higher and gaps are low, the loss of foliage due to seasonality creates a large increase in the number and size of gaps detected. The disproportionate increase in gaps being detected by the LiDAR results in all drainage classes having the same proportion of gaps.

To account for this inequity in areas, estimates of gaps per hectare in each drainage class were also calculated. Across the three polygons, the estimate of gaps per hectare was higher in the poorly drained areas and decreased as drainage improved. Additionally, the mean gap size decreased as drainage improved. Overall, these results show that gaps will be more prevalent in areas of poor drainage than in better drained areas. In addition, gaps are larger in the poorly drained areas in the better drained areas.

The lack of replication within the cover classes prevented an analysis of variance from being conducted which could have provided more insight into how gap frequency or size differs between drainage classes. While there were two aspen polygons in this analysis, the seasonal difference between the LiDAR scans prevented any further analysis at the gap level. Using the DTW values and canopy cover classifications for each pixel, a logistic regression was run for each polygon to determine if DTW could be used to predict canopy cover. While the results were statistically significant, the receiver operating curves (ROC) did not have values higher than 0.60 (results not shown). According to Hosmer and Lemeshow (2000), values between 0.5 and 0.7 indicate poor discrimination; values between 0.7 and 0.8 indicated moderate discrimination; and values higher than 0.9 indicate excellent discrimination. One explanation for the lack of predictive ability in these results may be that within any gap, there is a transition in DTW from the lowest point to the highest point. Each gap can therefore have several drainage classes with the poorest in the minority. From a practical perspective, knowing the probability of a single gap being a gap is of marginal value since gaps are clusters of pixels. The summary tables using the minimum DT to classify gaps into DTW showed the key trends that we expected.

4.4.2 Occurrence of Wet Areas

In the field, the wet areas in each polygon were mostly narrow, intermittent streams, although there were several ephemeral draws that also appeared as wet areas according to WAM. The centers of the stream channels likely correspond to the linear groups of pixels classified as having very poor drainage. With the channels being bordered by pixels classified as poor, imperfect, and moderately well, we can likely estimate the width of the stream channels depending on the severity of seasonal flooding. The addition of a digital elevation model (DEM)

layer may assist in visualizing stream channels and areas that can flood beyond what is seen in the raster images and provide additional ways to estimate the width of stream channels.

Although stream channels may be considered by some to be areas unable to host trees, they were not removed from the merchantable area of the polygons in this study. In these polygons, stream channels were generally too narrow to prevent trees from closing the canopy above them. With canopy cover being our main indicator of merchantability it was not apparent how the stream channels affected the trees. The use of additional WAM products such as the flow accumulation and flow direction layers could be explored to determine how canopy cover is affected by wet areas. Operationally, streams of a given size would be buffered and the area removed from the merchantable land base.

4.4.3 Raster processing

In this chapter, the CHM was processed in raster format to estimate gap areas, while in Chapters 2 and 3, a vector model created from the CHM was used. This resulted in a difference in merchantable gap area estimates between the two models, with the raster models having larger merchantable gap estimates between 0.78 ha and 2.91 ha. This difference can be attributed to the simplification that occurs when a raster model is converted to a vector. Initially, the vector models of the CHMs were used in Chapters 2 and 3 because they provided better estimates of where the gap boundaries may be when assessing the gaps in the field. Processing the gaps as raster models in this chapter allowed for easier integration with the DTW raster layers. With both versions of the CHM being effective in providing estimates of gap area, more work to assess the differences in accuracy of the two versions of a CHM is suggested.

During the creation of the raster that combined both the CHM and DTW rasters, the CHM had a resolution of 3 m^2 while the DTW raster had a resolution of 1 m^2. This difference in resolution, along with differences in the raster boundaries, results in a loss of resolution in the new combined raster. In cases where raster resolutions are different, ArcGIS 10.1 creates rasters at the resolution of the largest raster pixels involved. In the case of this study, the product rasters were created at a 3 m^2 resolution. The difference in boundaries also means that the pixels are not perfectly aligned with nine DTW pixels corresponding to each CHM pixel. To account for this, the pixel in the DTW layer closest to the center of each CHM pixel is used to determine the depth to water in the product raster. With gradients between pixels in the DTW layer being very gradual any reprocessing of the DTW layer at a 3 m^2 pixel was not considered necessary and would likely still result in some misalignment between the two rasters.

4.4.4 Application

The ability to add new layers of data to the CHM offers opportunities for better forest management decision making. When considering the addition of the DTW layer, it becomes apparent that gaps are larger and more prevalent in areas with poor and very poor drainage. Forest planners may consider removing the merchantable gaps in the very poor and poor drainage classes from their merchantable land base knowing that the forest in these areas are likely low in yield due to the gaps, and may be difficult to regenerate. For the polygons in this study, the low proportion of wet areas would affect the potential volume estimates calculated in Chapter 3 to only a small degree, reducing the potential growing area by between 0.21 and 1.69 ha across the four polygons. This is unlikely to affect volume predictions at this scale to any great degree. However, if persistent gaps were recognizable for an entire stratum, this may prevent an overestimation of predicted volume. Further work on discerning temporary gaps from persistent gaps may be an important next step in gap research.

Reducing the predicted volume based on wet areas can be further justified based on ecological reasons. Beyond the low stocking that is caused by gaps, wet areas may have different, less desirable species than the drier areas of the polygon. For example, in aspen dominated polygons, wet areas often feature a higher proportion of balsam poplar (Populus balsamifera L.). In harvest operations, balsam poplar is less merchantable than aspen in that it rots sooner and has a shorter lifespan (Peterson and Peterson, 1992). From an operational perspective, harvesting in these areas is less profitable than in the drier, more fully stocked pure aspen fragments. In addition, the harvest of wet areas often results in more difficult silviculture and can be subject to rutting by heavy machinery if summer harvesting is done. With Alberta harvest regulations requiring buffering of certain areas prior to harvest and the additional sensitivity of wet areas being acknowledged, the use of WAM in providing harvest boundaries within a forest polygon may both reduce the expense per hectare of harvest and silviculture and protect the sensitive areas.

The inclusion of additional layers to a CHM can also be effective beyond the use of WAM. The inclusion of layers that classify soil types, the forest overstory or understory, or other forest characteristics may allow further inferences to be made about the forest canopy and gaps, as well as about productivity, biodiversity and other values. Another important avenue that should be explored is the ability to classify gap dynamics, to study the temporal nature of gaps. Repeated LiDAR flights could help understand how gaps change over time (Vepakomma *et al*., 2008). This may further improve our understanding of gap dynamics and further improve estimates of potential polygon volume beyond those estimated using the procedures in Chapter 3.

4.5 Conclusions

With the ability to understand and classify gaps according to the local soil conditions, I have demonstrated how we can potentially improve forestry at both the planning stage and during harvest operations. There are numerous data layers similar to WAM that can be added to a LiDAR layer to further our ability to make inferences about gaps and gap dynamics for a number of disciplines.

References

Bouget, C., and Duelli, P. 2004. The effects of windthrow on forest insect communities: a literature review. Biological Conservation **118(3):** 281 – 299. doi: 10.1016/j.biocon.2003.09.009

Chavez, V., and Macdonald, S.E. 2010. The influence of canopy patch mosaics on understory plant community composition in boreal mixedwood forest. Forest Ecology and Management **259(6):** 1067 – 1075. doi: 10.1016/j.foreco.2009.12.013

Cumming, S.G., Schmiegelow, F.K., and Burton, P.J. 2000. Gap dynamics in boreal aspen stands: is the forest older than we think? Ecological Applications **10(3):** 744–759. doi: 10.2307/2641042

Hosmer, D.W. and Lemeshow, S. 2000. Applied Logistics Regression, Second Edition. John Wiley and Sons Inc. 383 pp.

MacIsaac, D., Comeau, P.G., and Macdonald, S.E. 2006. Dynamics of regeneration gaps following harvest of aspen stands. Canadian Journal of Forest Research **36(7):** 1818 – 1833. doi: 10.1139/X06-077

Murphy, P.N.C., Ogilvie, J., Men, F.-R., White, B., Bhatti, J.S., and Arp, P.A. 2011. Modelling and mapping topographic variations in forest soils at high resolution: A case study. Ecological Modelling **222(14):** 2314 – 2332. doi: 10.1016/j.ecolmodel.2011.01.003

Peterson, E.B., and Peterson, N.M. 1992. Ecology, management and use of aspen and balsam poplar in the prairie provinces, Canada. Forestry Canada, Northern Forestry Center. Special Report 1.

Runkle, J.R. 1992. Guidelines and sample protocol for sampling forest gaps. USDA Forest Service General Technical Report PNW-GTR-293.

Tansanu, C.S. 2007. The Role of Forest Stand Structure in Predicting Yield. M.Sc Thesis. University of Alberta. 129 pp.

Vepakomma, U., St-Onge, B., and Kneeshaw, D. 2008. Spatially explicit characterization of boreal forest gap dynamics using multi-temporal LiDAR data. Remote Sensing of Environment **112(5):** 2326 – 2340. doi: 10.1016/j.rse.2007.10.001

White, B., Ogilvie, J., Campbell, D.M.H., Hiltz, D., Gauthier, B., Chisholm, H.K., Wen, H.K., Murphy, P.N.C., and Arp, P.A. 2012. Using the cartographic depth-to-water index to locate small streams and associated wet areas across landscapes. Canadian Water Resources Journal **37(4):** 333 -347. doi: 10.4296/cwrj2011-909

Chapter 5: General Conclusions

This thesis examines methods that can be used to process LiDAR point cloud data for the purposes of delineating canopy gaps, with a goal of improving forest management practices. The objective was to determine whether gap delineation methods developed for other forest types in Europe (*e.g.* Gaulton and Malthus, 2010) could be applied in the boreal forests of Alberta using LiDAR data currently made available by the Alberta Ministry of Environment and Sustainable Resource Development.

The first objective of Chapter 2 was to develop canopy height models (CHMs) from the LiDAR point cloud for each of the research polygons. Our second objective was to develop mathematical models that relate the LiDAR gap areas derived from the CHM to field measured expanded gap measurements (Runkle, 1982). With the main objectives of this thesis relating to forest volume loss, gap definition was linked to the minimum height of a merchantable tree. For other applications, the definition used can be modified.

The results from the LiDAR analysis show that within a polygon, the frequency distribution of gap sizes was an inverse J-shape, with many small gaps and fewer large gaps. However, the small gaps made up only a small proportion of total gap area, while the few large gaps made up a much larger proportion of the total gap area. The minimum gap size that could be detected was driven by the resolution of the canopy height model. Choosing the correct pixel size was an important step as a small pixel size was too sensitive in detecting gaps and a large pixel size had the potential to miss gaps. The pixel size also needed to work well with the LiDAR point cloud density. Additionally, between the two aspen polygons, one was flown leaf on and one was flown leaf off, and this also had to be considered when selecting the appropriate pixel size. Having polygons available with flights during different seasons aids in determining the sensitivity of the LiDAR in detecting gaps.

The models developed to relate the LiDAR gaps to expanded gaps were statistically significant and had strong model fit (R^2) values. The fact that each stand was represented by a significantly different equation demonstrates the importance of seasonality with deciduous species. The power functions behave better biologically, however, further analysis of the relationship between LiDAR gaps and expanded gaps is needed for both very small gaps (<100 m^2) and for larger gaps (>400 m^2). While the number of small gaps in a polygon is large, identifying these gaps in the field is difficult because they may not be readily apparent and measuring their small size requires precise measurements. For the larger gaps, the number found within a single polygon will be limited, so understanding the how large LiDAR gaps relate to

field measurements may require measurements from several polygons. Additionally, large gaps can have islands of trees within them, thus they can be difficult to measure. The understanding of the relationship between LiDAR gap and expanded gap for large gaps may not be as important as small and mid-sized gaps since the ratio of crown overhang to overall gap size is small.

In Chapter 3, the LiDAR gap areas were applied to the expanded gap models that had been developed in Chapter 2 to understand how gaps affect the potential volume within a polygon. Using field measurements, estimates of how much expanded gap area a merchantable canopy tree requires were made by measuring expanded occupancy from a sample of trees in fully stocked areas, using measurement methods similar to Runkle's expanded gap (Runkle, 1982). The area represented the expanded gap area a single merchantable tree occupied in a fully stocked portion of the polygon. These estimates of expanded occupancy were then applied to estimate how many merchantable trees could potentially be added to each gap within a polygon. This provided an estimate of the potential volume of a polygon when no gaps were present, as well as an estimate of the volume lost to gaps. To achieve this, crowns were assumed to be circular and would be equidistant from one another. Importantly, this process identified the minimum size of an expanded gap that was needed to host a merchantable tree. All gaps below this threshold were considered to be interstitial spaces between trees and not included in the potential volume estimates. To assess whether the potential volume estimates were realistic, we compared the volume per hectare estimates from temporary sample plots placed in near fully stocked fragments of the polygon (Tansanu, 2007) to our potential volume estimates. The results showed that the methodology was robust and results were plausible. The main application of this research deals with estimating the potential volume for a polygon. Traditional forest practices estimate average yield based on a random sample of temporary sample plots. Using with GIS and LiDAR estimates of how much a polygon should yield based on the percentage of area unoccupied by trees can be made. Forest operators will also be able to better predict harvest volumes brought to the mill. Forest growth and yield modellers can utilize the percentage of gaps to further improve future yield estimates by accounting for gaps. Further development of these relationships to account for the seasonality of deciduous polygons across a landscape would be useful, as LiDAR scans are not necessarily conducted during the same season in a single region.

The objectives of Chapter 4 were to then add an additional data layer to the GIS, in the form of a depth to water index layer, to see if further information could be used to understand individual gaps. In this chapter, I developed raster filtering methods to remove small gaps from the CHMs, and then determined how prevalent gaps were within different drainage classes. The results showed that in areas with poor soil drainage, gaps were more prevalent and larger, while

in areas that were well drained gaps were less prevalent and smaller. This suggests that the addition of additional GIS layers to an analysis should allow for improved characterization of the nature and frequency of individual gaps. Further research to understand the gaps in each drainage class would be useful, as gaps in poorly drained soils have a likelihood of being persistent (MacIssac et al., 2006). Operationally, understanding why gaps are present can lead to better forest management decision making. Gaps found in low lying draws may indicate sensitive sites that may pose difficulties in regeneration. Having this information in advance of harvesting would lead to better forest management.

In this thesis, I have moved from sampling gaps to total enumeration of gaps within a polygon. The processes developed in this study can be used over an entire landscape. By stratifying polygons into meaningful groups based on characteristics such as species, age and location, a broad understanding of how gaps span the landscape can be drawn. LiDAR scans taken at two different periods in time may also provide useful information on gap dynamics.

References

Gaulton, R., and Malthus, T.J. 2010. LiDAR mapping of canopy gaps in continuous cover forests: A comparison of canopy height model and point cloud based techniques. International Journal of Remote Sensing **31(5):** 1193 – 1211. doi: 10.1080/01431160903380565

MacIsaac, D., Comeau, P.G., and Macdonald, S.E. 2006. Dynamics of regeneration gaps following harvest of aspen stands. Canadian Journal of Forest Research **36(7):** 1818 – 1833. doi: 10.1139/X06-077

Runkle, J.R. 1982. Patterns of disturbance in some old-growth mesic forests of eastern North America. Ecology **63(5)**: 1533–1546. doi: 10.2307/1938878

Tansanu, C.S. 2007. The Role of Forest Stand Structure in Predicting Yield. M.Sc Thesis. University of Alberta. 129 pp.

Appendices

Appendix A

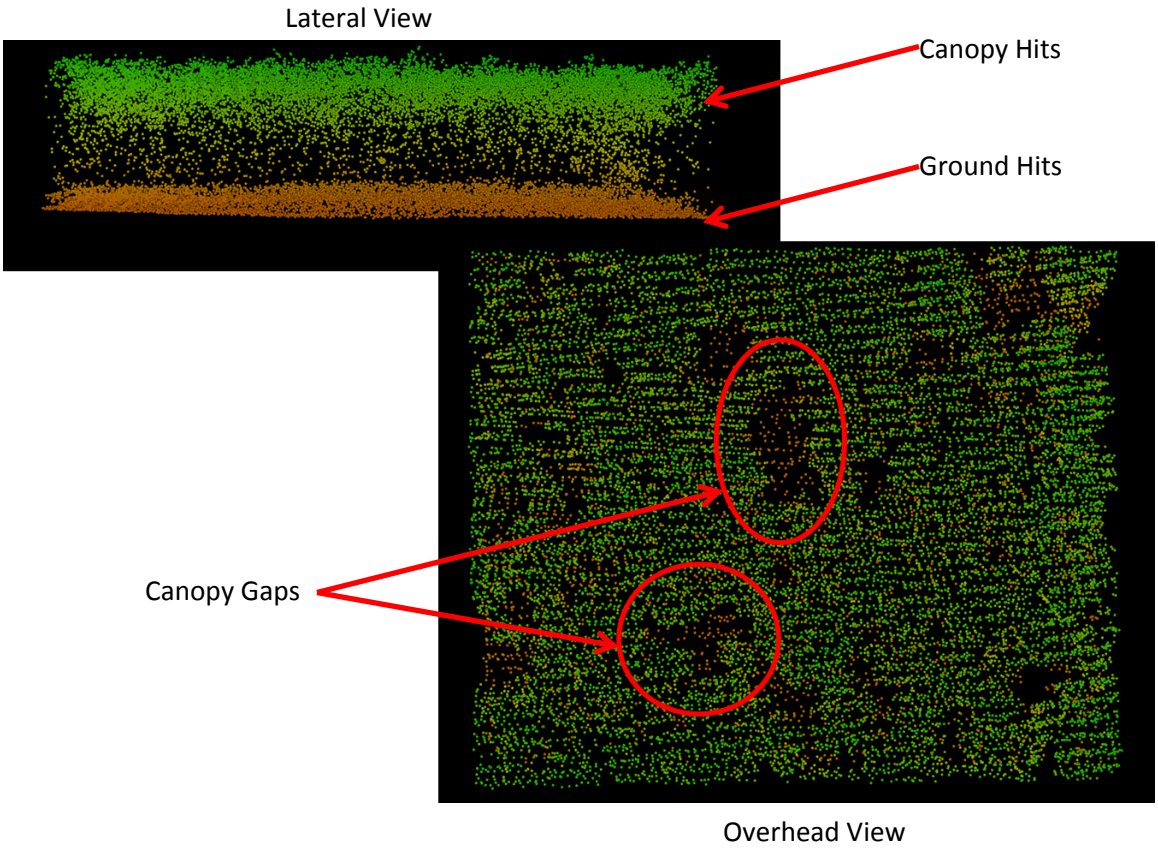

Appendix A: Images of the raw point cloud from lateral and overhead views. The lateral view displays the distinction between canopy and ground hit seen by the LiDAR. The overhead view shows that in areas with no canopy cover that gaps are clearly displayed.

Appendix B

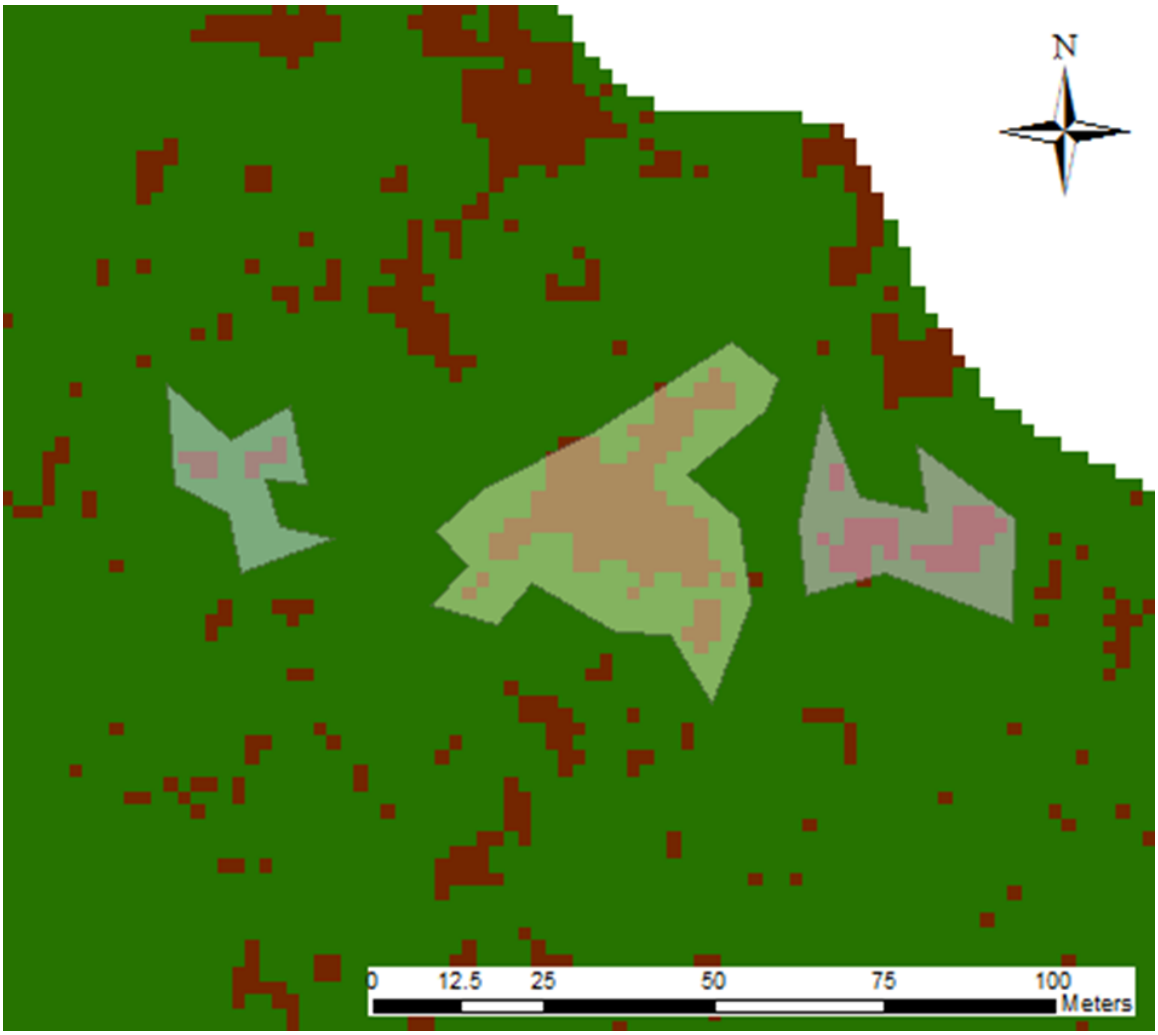

Appendix B: A canopy height model (CHM) raster which depicts canopy pixels in green and gap pixels in brown. Expanded gap polygons have been overlaid to show the differences in predicted area from the CHM and the expanded gap areas measured in the field.

Appendix C

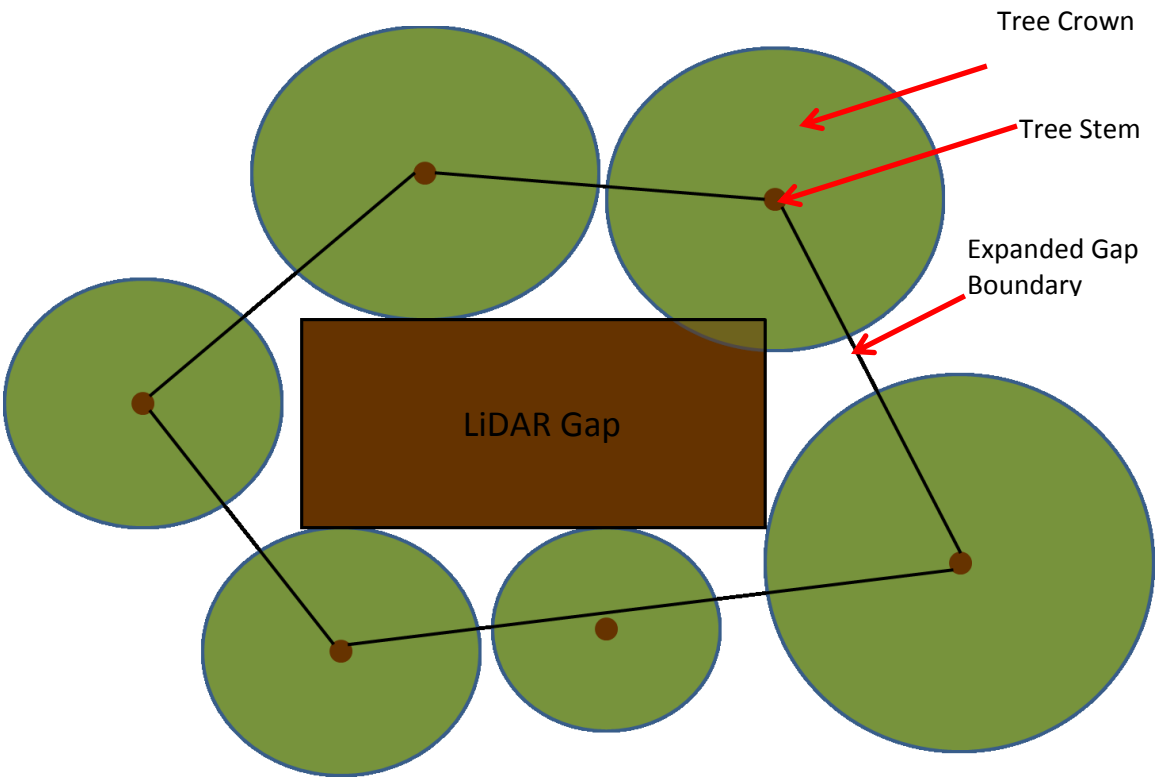

Appendix C: Schematic of the forest canopy depicting a LiDAR gap surrounded by canopy trees. The polygon created by the tree stems bordering the LiDAR gap act as vertices of the expanded gap polygon.

Appendix D

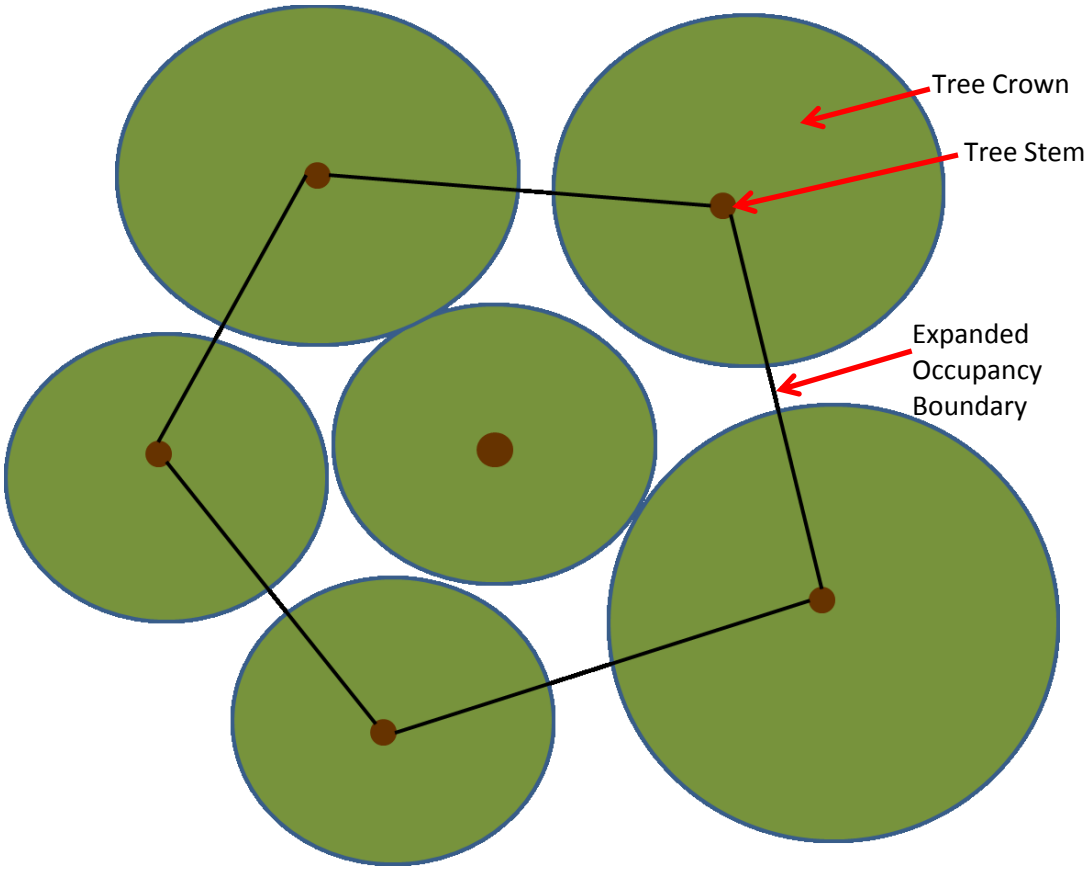

Appendix D: Schematic of the forest canopy depicting a fully enclosed canopy tree surrounded by neighbouring trees. The polygon created by the tree stems bordering the center tree as vertices of the expanded occupancy polygon.

Bibliography

Alberta Land and Forest Service. 1994. Permanent sample plot field procedures manual. Alberta Land and Forest Service, Forest Management Division, Forest Measurement Section. Edmonton, Alberta.

Alberta Sustainable Resource Development. 2005. Alberta vegetation inventory interpretation standards. Version 2.1.1. Alberta Sustainable Resource Development, Resource Information Management Branch.

BC Ministry of Forests. 1998[a]. OAF1 Project Report #1. An overview of stocking gaps and OAF1 estimates for TIPSY. B.C. Ministry of Forests, Forest Practices Branch. Victoria, B.C.

BC Ministry of Forests. 1998[b]. OAF1Project Report #2. Ground-based survey method. B.C. Ministry of Forests, Forest Practices Branch. Victoria, B.C.

B.C. Ministry of Forests, Lands and Natural Resource Operations. A Table Interpolation Program for Stand Yields (TIPSY), Version 4.3. Ministry of Forests, Lands and Natural Resource Operations, Forest Analysis and Inventory Branch, Victoria B.C, Canada. **2013**. Available online: http://www.for.gov.bc.ca/hre/software/download.htm (accessed on 30 December 2014).

Bokalo, M.; Stadt, K.J.; Comeau, P.G.; Titus, S.J. Mixedwood Growth Model (MGM) (version MGM2010.xls). University of Alberta, Edmonton, Alberta, Canada. **2010**. Available online: http://www.rr.ualberta.ca/Research/MixedwoodGrowthModel.aspx (accessed on 20 November 2014).

Bouget, C., and Duelli, P. 2004. The effects of windthrow on forest insect communities: a literature review. Biological Conservation **118(3):** 281 – 299. doi: 10.1016/j.biocon.2003.09.009

Bray, J.R. 1956. Gap Phase Replacement in a Maple-Basswood Forest. Ecology **37(3):** 598 – 600. doi: 10.2307/1930185

Brokaw, N.V.L. 1982. The definition of treefall gap and its effect on measures of forest dynamics. Biotropica **14(2):** 158 – 160. doi: 10.2307/2387750

Brokaw, N.V.L. 1985. Gap-phase regeneration in a tropical forest. Ecology **66(3):** 682 – 687. doi: 10.2307/1940529

Chavez, V., and Macdonald, S.E. 2010. The influence of canopy patch mosaics on understory plant community composition in boreal mixedwood forest. Forest Ecology and Management **259(6):** 1067 – 1075. doi: 10.1016/j.foreco.2009.12.013

Comeau, P.G., Filipescu, C.N., Kabzems, R., and Delong, C. 2009. Corrigendum to: Growth of white spruce underplanted beneath spaced and unspaced aspen stands in northeastern B.C. – 10 year results. Forest Ecology and Management **257(7):** 1629 – 1636. doi: 10.1016/j.foreco.2009.01.025

Cumming, S.G., Schmiegelow, F.K., and Burton, P.J. 2000. Gap dynamics in boreal aspen stands: is the forest older than we think? Ecological Applications **10(3):** 744–759. doi: 10.2307/2641042

De Grandpre, L., Boucher, D., Bergeron, Y. and Gagnon, D. 2011. Effects of small canopy gaps on boreal mixedwood understory vegetation dynamics. Community Ecology **12(1):** 67 – 77. doi: 10.1556/ComEc.12.2011.1.9

Denslow, J.S., Schultz, J.C., Vitousek, P.M., and Strain, B.R. 1990. Growth responses of tropical shrubs to treefall gap environments. Ecology **71(1):** 165 – 179. doi: 10.2307/1940257

Eriksson, H. 1962. A comparison between the yield figures for permanent sample plots and those for the stand as a whole. Royal College of Forestry, Department of Forest Yield and Research. Research Notes Nr:14. 72 pp. Printed in Swedish with English summary.

Frankin, J.F., Shugart, H.H., and Harmon, M.E. 1987. Tree death as an ecological process. Bioscience **37(8):** 550 – 556. doi: 10.2307/1310665

Fukui, D., Hirao, T., Murakami, M., and Hirakawa, H. 2011. Effects of treefall gaps created by windthrow on bat assemblages in a temperate forest. Forest Ecology and Management **261(9):** 1546 – 1552. doi: 10.1016/j.foreco.2011.02.001

Fuller, R.J. 2000. Influence of treefall gaps on distributions of breeding birds within interior old-growth stands in Bialowieża Forest, Poland. The Condor **102(2):** 267 – 274. doi: 10.1650/0010-5422(2000)102[0267:IOTGOD]2.0.CO;2

Gaulton, R., and Malthus, T.J. 2010. LiDAR mapping of canopy gaps in continuous cover forests: A comparison of canopy height model and point cloud based techniques. International Journal of Remote Sensing 31(5): 1193 – 1211. doi: 10.1080/01431160903380565

Hosmer, D.W. and Lemeshow, S. 2000. Applied Logistics Regression, Second Edition. John Wiley and Sons Inc. 383 pp.

Huang, S. 1994. Report #1: Individual tree volume estimation for Alberta: Methods of formulation and statistical foundations. Alberta Environmental Protection, Land and Forest Service, Forest Management Division.

Jonsson B.G., and Esseen, P.-A. 1990. Treefall disturbance maintains high bryophyte diversity in a boreal spruce forest. Journal of Ecology: **78(4):** 924 – 936. doi: 10.2307/2260943

Kneeshaw, D.D., and Bergeron, Y. 1998. Canopy gap characteristics and tree replacement in the southeastern boreal forest. Ecology: **79(3):** 783 – 794. doi: 10.1890/0012-9658(1998)079[0783:CGCATR]2.0.CO;2

Koukoulas, S. and Blackburn, G.A. 2004. Quantifying the spatial properties of forest canopy gaps using LiDAR imagery and GIS. International Journal of Remote Sensing **25(15):** 3049 – 3071. doi: 10.1080/01431160310001657786

Kuuluvainen, T. 1994. Gap disturbance, ground microtopography, and the regeneration dynamics of boreal coniferous forests in Finland – a review. Annales Zoologici Fennici **31(1):** 35 – 51.

Long, J.N. and Smith, F.W. 1992. Volume increment in *Pinus contorta* var. *latifolia*: the influence of stand development and crown dynamics. Forest Ecology and Management **53(1-4):** 53-64. doi: 10.1016/0378-1127(92)90033-6

MacIsaac, D., Comeau, P.G., and Macdonald, S.E. 2006. Dynamics of regeneration gaps following harvest of aspen stands. Canadian Journal of Forest Research **36(7):** 1818 – 1833. doi: 10.1139/X06-077

McCarthy, J. 2001. Gap dynamics of forest trees: A review with particular attention to boreal forests. Environmental Reviews **9(1)**: 1 – 59. doi: 10.1139/er-9-1-1

McGaughey, R.J. Fusion/LDV – Version 3.41. Build Date Jan 28, 2014. United States Department of Agriculture - Forest Service, Pacific Northwest Research Center

Murphy, P.N.C., Ogilvie, J., Men, F.-R., White, B., Bhatti, J.S., and Arp, P.A. 2011. Modelling and mapping topographic variations in forest soils at high resolution: A case study. Ecological Modelling **222(14):** 2314 – 2332. doi: 10.1016/j.ecolmodel.2011.01.003

Naesset, E. 1997. Determination of mean tree height of forest stands using airborne laser scanner data. ISPRS Journal of Photogrammetry & Remote Sensing **52(2):** 49 – 56. doi: 10.1016/S0924-2716(97)83000-6

Peterson, E.B., and Peterson, N.M. 1992. Ecology, management and use of aspen and balsam poplar in the prairie provinces, Canada. Forestry Canada, Northern Forestry Center. Special Report 1.

Pretzsch, H. 2014. Canopy space filling and tree crown morphology in mixed-species stands compared with monocultures. Forest Ecology and Management **327:** 251 – 264. doi: 10.1016/j/foreco.2014.04.027

Reutebuch, S.E., Andersen, H.-E., and McGaughey, R.J. 2005. Light detection and ranging (LIDAR): an emerging tool for multiple resource inventory. Journal of Forestry **103(6):** 286 – 292.

Runkle, J.R. 1982. Patterns of disturbance in some old-growth mesic forests of eastern North America. Ecology **63(5)**: 1533–1546. doi: 10.2307/1938878

Runkle, J.R. 1992. Guidelines and sample protocol for sampling forest gaps. USDA Forest Service General Technical Report PNW-GTR-293.

Sattler, D.F., Comeau, P.G., and Achim, A. 2014. Branch models for white spruce (*Picea glauca* (Moench) Voss) in naturally regenerated stands. Forest Ecology and Management **325:** 74 – 89. doi: 10.1016/j.foreco.2014.03.051

Schliemann, S.A., and Bockheim, J.G. 2011. Methods for studying treefall gaps: A review. Forest Ecology and Management **261(7):** 1143 – 1151. doi: 10.1016/j.foreco.2011.01.011

Stadt, K.J., Lieffers, V.J., Hall, R.J. and Messier, C. 2005. Spatially explicit modelling of PAR transmission and growth of *Picea glauca* and *Abies balsamea* in the boreal forests of Alberta and Quebec. Canadian Journal of Forest Research **35(1):** 1 – 12. doi: 10.1139/X04-141

Tansanu, C.S. 2007. The Role of Forest Stand Structure in Predicting Yield. M.Sc Thesis. University of Alberta. 129 pp.

Treitz, P., Lim, K., Woods, M., Pitt, D., Nesbitt, D., and Etheridge, D. 2012. LiDAR sampling density for forest resource inventories in Ontario, Canada. Remote Sensing **4(4):** 830 – 848. doi: 10.3390/rs4040830

Vehmas, M., Packalen, P., Matlamo, M., and Eerikainen, K. 2011. Using airborne laser scanning data for detecting canopy gaps and their understory type in mature boreal forest. Annals of Forest Science **68(4):** 825 – 835. doi: 10.1007/s13595-001-0079-x

Vepakomma, U., St-Onge, B., and Kneeshaw, D. 2008. Spatially explicit characterization of boreal forest gap dynamics using multi-temporal LiDAR data. Remote Sensing of Environment **112(5):** 2326 – 2340. doi: 10.1016/j.rse.2007.10.001

Watt, A.S. 1947. Pattern and Process in the Plant Community. Journal of Ecology **35 (1 and 2):** 1 – 22. doi: 10.2307/2256497

White, B., Ogilvie, J., Campbell, D.M.H., Hiltz, D., Gauthier, B., Chisholm, H.K., Wen, H.K., Murphy, P.N.C., and Arp, P.A. 2012. Using the cartographic depth-to-water index to locate small streams and associated wet areas across landscapes. Canadian Water Resources Journal **37(4):** 333 -347. doi: 10.4296/cwrj2011-909